Cellular/Molecular

Regulation of Early Neurite Morphogenesis by the Na^+/H^+ Exchanger NHE1

Wun-Chey Sin,[1]* David M. Moniz,[1]* Mark A. Ozog,[1] Jessica E. Tyler,[1] Masayuki Numata,[2] and John Church[1,3]

Departments of [1]Cellular and Physiological Sciences and [2]Biochemistry and Molecular Biology and [3]Graduate Program in Cell and Developmental Biology, The University of British Columbia, Vancouver, British Columbia V6T 1Z3, Canada

The ubiquitously expressed Na^+/H^+ exchanger NHE1 plays an important role in regulating polarized membrane protrusion and directional motility in non-neuronal cells. Using NGF-differentiated PC12 cells and murine neocortical neurons *in vitro*, we now show that NHE1 plays a role in regulating early neurite morphogenesis. NHE1 was expressed in growth cones in which it gave rise to an elevated intracellular pH in actively extending neurites. The NHE1 inhibitor cariporide reversibly reduced growth cone filopodia number and the formation and elongation of neurites, especially branches, whereas the transient overexpression of full-length NHE1, but not NHE1 mutants deficient in either ion translocation activity or actin cytoskeletal anchoring, elicited opposite effects. In addition, compared with neocortical neurons obtained from wild-type littermates, neurons isolated from NHE1-null mice exhibited reductions in early neurite outgrowth, an effect that was rescued by overexpression of full-length NHE1 but not NHE1 mutants. Finally, the growth-promoting effects of netrin-1, but not BDNF or IGF-1, were markedly reduced by cariporide in wild-type neocortical neurons and were not observed in NHE1-null neurons. Although netrin-1 failed to increase growth cone intracellular pH or Na^+/H^+ exchange activity, netrin-1-induced increases in early neurite outgrowth were restored in NHE1-null neurons transfected with full-length NHE1 but not an ion translocation-deficient mutant. Collectively, the results indicate that NHE1 participates in the regulation of early neurite morphogenesis and identify a novel role for NHE1 in the promotion of early neurite outgrowth by netrin-1.

Introduction

The precise regulation of neurite morphogenesis is essential for the correct development and function of the CNS. Although a large number of environmental signals are known to regulate the formation and/or subsequent elongation and branching of neurites, much remains to be learned about the mechanisms involved in transducing these signals into the growth cone to reorganize the cytoskeleton and regulate neurite outgrowth.

The solute carrier family 9 includes nine mammalian Na^+/H^+ exchangers (NHE1–NHE9) that preferentially catalyze the electroneutral exchange of protons and sodium ions down their respective concentration gradients (Orlowski and Grinstein, 2004; Brett et al., 2005). The best studied of these isoforms is NHE1 (Sardet et al., 1989), which resides in the plasma membrane of virtually all cell types. NHE1 contains two functional domains, a relatively conserved N-terminal/transmembrane ion translocation domain and a C-terminal cytoplasmic regulatory domain that serves as a target for numerous factors that regulate transport activity (Orlowski and Grinstein, 2004). The C-terminal domain also has important structural roles, serving as a plasma membrane anchor for the actin cytoskeleton through its direct interaction with the ezrin, radixin, and moesin (ERM) family of actin-binding proteins and by acting as a scaffold for the assembly of macromolecular signaling complexes (for review, see Meima et al., 2007).

In addition to its established roles in regulating intracellular acid-base, electrolyte and volume homeostasis, NHE1 plays an important role in regulating growth and directed motility in a variety of non-neuronal cell types (Simchowitz and Cragoe, 1986; Cardone et al., 2005; Meima et al., 2007; Stock et al., 2008). In migrating cells, for example, NHE1 accumulates at the leading edge to regulate the dynamic reorganization of the actin cytoskeleton and polarized membrane protrusion, and reductions in ion translocation activity or mutations that disrupt actin cytoskeletal anchoring and thereby mislocalize NHE1 away from the leading edge impair directional motility (Grinstein et al., 1993; Denker et al., 2000; Klein et al., 2000; Lagana et al., 2000; Denker and Barber, 2002; Stüwe et al., 2007; Hayashi et al., 2008; Schneider et al., 2009).

The fact that neurite outgrowth involves cytoskeletal rearrangements at the growth cone in many respects similar to those underlying leading edge membrane protrusion in migrating non-neuronal cells (Song and Poo, 2001; da Silva and Dotti, 2002; Chhabra and Higgs, 2007) prompted us to examine the role of NHE1 in early neurite formation, extension, and branching.

Received April 29, 2009; accepted June 3, 2009.

This work was supported by Canadian Institutes of Health Research Grant MOP-77616. We thank D. L. Barber for gifts of plasmid DNA, Sanofi-Aventis for supplies of cariporide, G. Modha for designing the NHE1 genotype primers, and N. Tam for assistance with the measurements of neurite outgrowth.

*W.-C.S. and D.M.M. contributed equally to this work.

Correspondence should be addressed to John Church, Department of Cellular and Physiological Sciences, University of British Columbia, Life Sciences Centre, 2350 Health Sciences Mall, Vancouver, BC V6T 123, Canada. E-mail: jchurch@interchange.ubc.ca.

DOI:10.1523/JNEUROSCI.2030-09.2009

 0270-6474/09/298946-14$15.00/0

Materials and Methods

Reagents. Cariporide (HOE642), a gift from Sanofi-Aventis, was dissolved in DMSO and was applied at 1 μM unless otherwise indicated. The following reagents were purchased from the given suppliers: 2′,7′-*bis*-(2-carboxyethyl)-5-(and-6)-carboxyfluorescein (BCECF) AM (Invitrogen), 5-(*N*-ethyl-*N*-isopropyl)-amiloride (EIPA) (Sigma-Aldrich), anti-glyceraldehyde-3-phosphate dehydrogenase (GAPDH) antibody (HyTest), Alexa Fluor 488- and 568-conjugated phalloidin (Invitrogen), anti-vinculin and anti-MAP2 antibodies (Sigma-Aldrich), anti-hemagglutinin (HA) antibody (Covance), anti-NHE1 antibody (BD Biosciences), recombinant mouse insulin-like growth factor-1 (IGF-1; Stem Cell Technologies), and recombinant mouse netrin-1 and recombinant human brain-derived neurotrophic factor (BDNF) (R & D Systems).

Cell culture. Unless noted, cell culture media and supplements were obtained from Invitrogen. PC12 cells (American Type Culture Collection) were maintained in 60 mm plastic tissue culture plates at 37°C under a 5% CO_2 atmosphere in high-glucose DMEM with GlutaMAX supplemented with 10% horse serum, 5% fetal bovine serum (FBS), 100 U/ml penicillin, and 100 μg/ml streptomycin (Sigma-Aldrich). For differentiation, PC12 cells were seeded at a low density of 2×10^4 cells/ml on glass coverslips coated with collagen (Millipore) and treated for up to 72 h with nerve growth factor (NGF) at 50 ng/ml (Cedarlane Laboratories) in high-glucose DMEM with GlutaMAX supplemented with 1% FBS and penicillin/streptomycin (medium was replaced every 24 h with fresh NGF-containing medium). Neocortical neurons were isolated from either embryonic day 16 (E16) wild-type (WT) C57BL/6 mice (Charles River Laboratories) or postnatal day 0.5 (P0.5) *Nhe1* homozygous mutant (*NHE1*$^{-/-}$), heterozygous (*NHE1*$^{+/-}$), and wild-type (*NHE1*$^{+/+}$) littermate progeny of matings between heterozygous B6.SJL, +/*swe* mice (The Jackson Laboratory), which harbor a spontaneous mutation in the *Nhe1* allele (Cox et al., 1997). In the latter cases, animals were killed within 12 h of birth, and genotyping was performed on brain tissue as described previously (Xue et al., 2003) using the following primers: sense, 5′-CACTCTCTGCATCCCTCCTC-3′ and antisense, 5′-AAGTCATGCGGCAAGCTAGT-3′, corresponding to base pairs 47312-47331 and 47956-47977 of the intronic region of the mouse NHE1 cDNA sequence (GenBank accession number BC052708). To isolate neocortical neurons, cortices freed of meninges were placed in ice-cold (4°C) HBSS supplemented with 10% FBS and penicillin/streptomycin and gently triturated with fire-polished Pasteur pipettes of diminishing tip diameter. The cell suspension was passed through a 70 μm cell strainer (BD Biosciences), and cells were subsequently resuspended in a 1:1 mixture of HBSS and plating medium [Neurobasal medium and DMEM/F-12 (3:2) supplemented with 10% FBS and penicillin/streptomycin]. To minimize synaptic interactions and ensure accurate morphometric analyses, neurons were plated at low density (1×10^5 cells/cm^{-2}) on poly-D-lysine/laminin-coated two-well culture slides (BD Biosciences) and maintained for 72 h at 37°C under a 5% CO_2 atmosphere in Neurobasal medium and DMEM/F-12 (3:2) containing 2% B27 and penicillin/streptomycin. The culture medium was fully changed at 2 h after plating and thereafter half-changed every 24 h with fresh medium. All procedures involving mice conformed to guidelines established by the Canadian Council on Animal Care and were approved by The University of British Columbia Animal Care Committee.

DNA constructs and transfection procedures. The expression vectors phosphorylated cytomegalovirus (pCMV) and pCMV–NHE1–HA have been described previously (Orlowski, 1993; Denker et al., 2000). HA-tagged NHE1 mutants deficient in either ion translocation activity (NHE1–E266I$_{HA}$) or ERM binding (NHE1–KR/A$_{HA}$) (Denker et al., 2000) were generously provided by Dr. D. L. Barber (University of California, San Francisco, San Francisco, CA). A second HA-tagged NHE1 mutant with disrupted ERM binding (NHE1–Δ556–564$_{HA}$) was made using the Quick Change Site-Directed Mutagenesis kit (Stratagene) using pCMV–NHE1–HA as the template and the following primers: sense 5′-CACTGGAAGGACAAGCTCAACTGTCTAATAGCTGGAGAGCGCTCC-3′ and antisense 5′-GGAGCGCTCTCCAGCTATTAGACAGTTGAGCTTGTCCTTCCAGTG-3′. All cDNAs were verified by DNA sequencing, and the Na^+/H^+ exchange activity of each mutant was assessed in NHE-deficient PS120 fibroblasts cotransfected with phosphorylated enhanced green fluorescent protein–C1 (supplemental Figs. 1, 3, available at www.jneurosci.org as supplemental material). PC12 cells and mouse neocortical neurons were transiently transfected using Fugene 6 (Roche Applied Science) according to the instructions of the manufacturer. Anti-HA immunostaining was used to identify transiently transfected cells expressing high levels of exogenous full-length or mutant NHE1s, and only these cells were accepted for morphological analyses.

Immunocytochemistry. PC12 cells and mouse neocortical neurons were fixed for 10 min at room temperature in 4% paraformaldehyde in PBS, washed twice with PBS, permeabilized with 0.2% Triton X-100 for 5 min, washed with PBS, blocked with 2% BSA in PBS for 30 min, and incubated with appropriate primary antibodies diluted in 1% BSA at 4°C overnight. After three washes in PBS, cells were incubated with either Alexa Fluor 488 secondary antibody and/or Alexa Fluor 568-conjugated phalloidin, or vice versa, for 60 min at room temperature, followed by three additional washes in PBS. Coverslips were mounted onto glass slides using Prolong Gold antifade reagent with 4′,6′-diamidino-2-phenylindole (Invitrogen) and examined using an Axioplan 2 imaging microscope (Carl Zeiss).

Morphometric analyses. Images of individual PC12 cells and neocortical neurons [3 d *in vitro* (div) unless otherwise noted] were captured from randomly chosen fields on a Carl Zeiss Axioplan 2 imaging microscope, blinded to treatment group, and traced using Carl Zeiss AxioVision software (version 4.2). We determined the number and cumulative length of primary neurites (i.e., neurites >10 μm in length emanating directly from the cell body) per cell, the number and cumulative length of neurite branches (i.e., second- and higher-order neurites >5 μm in length) per cell, and the total number and total cumulative length of all neurites per cell. For mouse neocortical neurons, analysis was restricted to neurons at the Stage 2/3 transition, before polarization and the formation of a distinct axon (Arimura and Kaibuchi, 2007). Each experiment was performed on at least three (usually more than five) different batches of PC12 cells or cultured neurons. Data are presented as means ± SEM, with the accompanying *n* value referring to the number of cells (or, in Figs. 4 and 9, growth cones) from which data were obtained. Unless noted, statistical comparisons were performed using Kruskal–Wallis one-way ANOVA on ranks and then Dunn's method for pairwise comparison, with significance assumed at the 5% level.

Protein isolation and Western blotting. PC12 cells confluent on a 60 mm plate (see Fig. 1*a*) or brain tissue from P0.5 mice (see Fig. 6*a*) were lysed in 500 μl of ice-cold extraction buffer (0.1% SDS, 1% IGEPAL, 0.5% Sarkosyl, 150 mM NaCl, and 50 mM Tris-HCl, pH 8.0) in the presence of MiniComplete protease (Roche Applied Science) and phosphatase (Sigma-Aldrich) inhibitors. After centrifugation at 10,000 × *g* for 10 min, protein concentration was determined using the BCA protein quantification kit (Thermo Fisher Scientific). Protein samples were boiled for 5 min in SDS sample buffer and separated on a 10% polyacrylamide gel. Subsequently, proteins were transferred to polyvinylidene difluoride membrane (Bio-Rad). After incubation with primary antibody at 4°C overnight and horseradish peroxidase-linked secondary antibody for 1 h at room temperature, detection was achieved with SuperSignal chemiluminescent substrate (Thermo Fisher Scientific) on x-ray film.

Growth cone intracellular pH measurements. Cells were loaded with the AM form of BCECF (0.3 μM for 30 min at room temperature), mounted in a temperature-controlled recording chamber, and continuously superfused at <1 ml/min with a HCO_3^-/CO_2-buffered medium containing the following (in mM): 125 NaCl, 3 KCl, 21.5 $NaHCO_3$, 1.5 NaH_2PO_4, 1.5 $MgSO_4$, 10 D-glucose, and 2 $CaCl_2$, pH 7.35 (after equilibration with 5% CO_2/95% air at 34°C). A low concentration of BCECF was used to avoid the potential dissipation of intracellular pH (pH_i) microdomains associated with higher (≥1 μm) concentrations of the fluorophore (Feijó et al., 1999). The dual-excitation ratio method was used to measure pH_i, using a Carl Zeiss Axioskop 2 FS plus microscope (Achroplan 100× objective, numerical aperture 1.25; Carl Zeiss), a DG-5 wavelength switcher (Sutter Instruments), and Slidebook digital microscopy software (version 4.2; Intelligent Imaging Innovations). Details of the methods used have been presented previously (Sheldon and Church, 2002). In brief, fluorescence

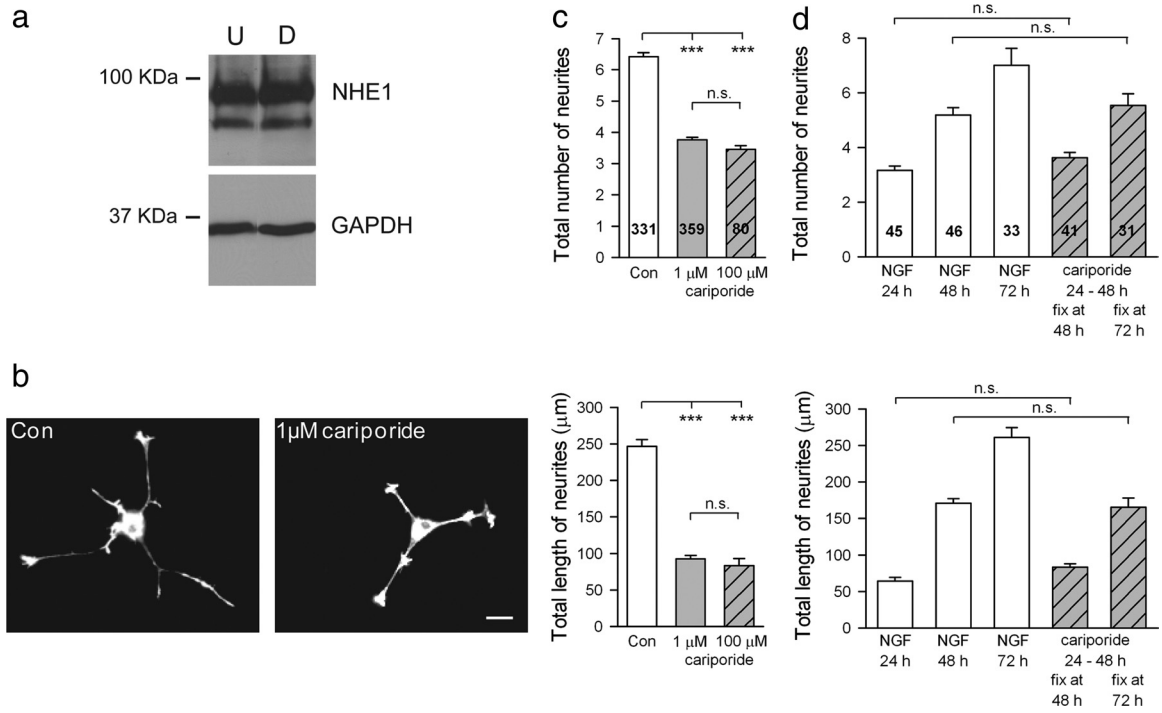

Figure 1. Inhibition of NHE1 reduces early neurite outgrowth in NGF-differentiated PC12 cells. ***a***, NHE1 is expressed in undifferentiated (U) and differentiated (D; 50 ng/ml NGF for 72 h) PC12 cells. Western blot analysis with anti-NHE1 antibody; GAPDH was used as a loading control. ***b***, Representative examples of PC12 cells differentiated with 50 ng/ml NGF for 72 h in the presence of cariporide vehicle (Con; 0.1% DMSO) or 1 μM cariporide. Cells stained with Alexa Fluor 488-conjugated phalloidin. Scale bar, 20 μm. ***c***, Quantification of the total number (top) and total cumulative length (bottom) of neurites per cell under the conditions shown on the figure. Compared with cells cultured in the presence of 0.1% DMSO (Con; white bars), early neurite outgrowth was reduced to a similar extent by 1 μM (gray bars) and 100 μM (gray hatched bars) cariporide. For all parameters measured, there were no significant differences between PC12 cells cultured in the absence versus presence of 0.1% DMSO (data not shown). ***d***, The effects of 100 μM cariporide on early neurite outgrowth are reversible. PC12 cells were differentiated with NGF for 24 h (column 1), 48 h (column 2), or 72 h (column 3) in the presence of cariporide vehicle (0.1% DMSO). Data in columns 4 and 5 are from parallel experiments in which 100 μM cariporide was applied from 24 to 48 h; cells were then either fixed at 48 h or maintained for an additional 24 h under cariporide-free conditions before fixation at 72 h. Quantitatively similar results were obtained with 1 μM cariporide (data not shown). In ***c*** and ***d***, experiments were conducted in parallel, all measured values are per cell, error bars represent SEM, and *n* values are shown in the columns. $^{***}p < 0.001$; n.s., not significant ($p > 0.05$).

emissions measured at 520 nm were detected with a cooled CCD camera (Retiga EXi; QImaging) and collected from regions of interest placed on individual growth cones and/or more proximal regions of neurites or cell bodies. To reduce photobleaching of the fluorophore and cell damage, neutral density filters were placed in the light path, and a high-speed shutter was used to limit light exposure to periods required for data acquisition. Raw emission intensity data at each excitation wavelength (495 and 440 nm) were corrected for background fluorescence before calculation of ratio values, which were typically acquired at 30 s intervals. To differentiate between stalled and actively extending neurites, the acquisition of every fourth BCECF-derived ratio pair was followed by the capture of a differential interference contrast (DIC) image; the latter were used to construct time-lapse image series, which were viewed offline. The one-point high-$[K^+]$/nigericin technique was used to convert background-corrected BCECF ratio emission intensity ratios into pH_i values. Parameters used in the calculation of pH_i values were derived from nonlinear least-squares regression fits to background-subtracted ratio versus pH data, which, in turn, were obtained in full *in situ* calibration experiments (Sheldon and Church, 2002); separate calibration parameters were used for data obtained from growth cones and more proximal regions of the cell (Rojas et al., 2006).

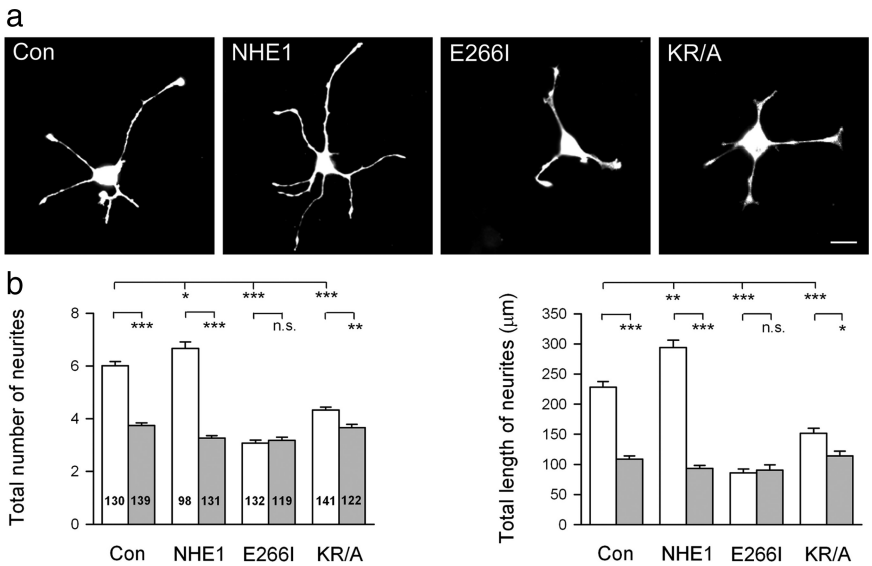

Figure 2. Ion translocation and ERM binding contribute to NHE1 regulation of early neurite outgrowth in NGF-differentiated PC12 cells. ***a***, Representative cells were either untransfected (Con) or transiently transfected with HA-tagged full-length NHE1 (NHE1), NHE1 lacking ion transport (E266I), or NHE1 lacking ERM binding (KR/A) and differentiated for 72 h with 50 ng/ml NGF. Untransfected and transfected cells stained with Alexa Fluor 488-conjugated phalloidin and anti-HA antibody, respectively. Scale bar, 20 μm. ***b***, Quantification of the total number (left) and total cumulative length (right) of neurites per cell in untransfected PC12 cells (Con) and PC12 cells overexpressing HA-tagged full-length NHE1, NHE1–E266I, or NHE1–KR/A, in the absence (white bars) or continuous presence (gray bars) of 1 μM cariporide. Experiments were conducted in parallel, all measured values are per cell, error bars represent SEM, and *n* values are shown in the columns. $^{*}p < 0.05$; $^{**}p < 0.01$; $^{***}p < 0.001$; n.s., not significant ($p > 0.05$). The separated measurements of changes in the numbers and cumulative lengths of primary neurites per cell and neurite branches per cell to the total values shown in ***b*** are presented in supplemental Figure 2 (available at www.jneurosci.org as supplemental material).

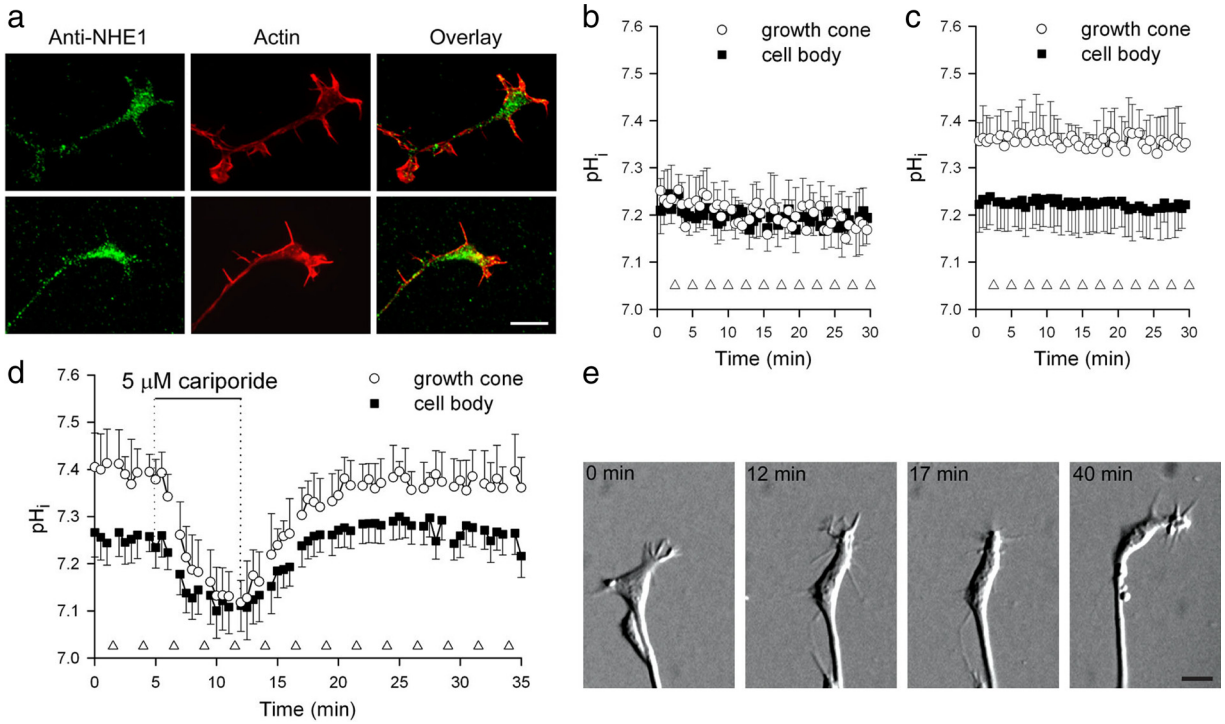

Figure 3. NHE1 is expressed in PC12 growth cones and influences their pH_i and morphology. ***a***, Representative growth cones from two different NGF-differentiated PC12 cells stained with anti-NHE1 antibody and Alexa Fluor 568-conjugated phalloidin. Scale bar, 10 μm. ***b***, ***c***, Simultaneous measurements of pH_i in growth cones (white circles) and somata and/or more proximal regions of primary neurites (black squares) in PC12 cells differentiated with 50 ng/ml NGF for 72 h. pH_i in growth cones of actively extending (***c***), but not stalled (***b***), neurites was consistently higher than in more proximal regions. $n = 10$ in all cases; error bars are SEM. White triangles indicate the time points at which DIC images were captured to identify actively extending neurites. ***d***, Cariporide (5 μM) caused reversible reductions in pH_i measured simultaneously in cell bodies and the growth cones of actively extending neurites. Records are the means of data obtained from eight PC12 cells on different coverslips; error bars are SEM. pH_i values measured in growth cones before (7.38 $\pm$ 0.05) and after recovery from cariporide (7.36 $\pm$ 0.05) were significantly higher than those measured simultaneously at cell bodies (7.25 $\pm$ 0.03 and 7.28 $\pm$ 0.05, respectively) ($p < 0.05$ in both cases by Student's *t* test). In contrast, at the end of the 7 min application of cariporide, pH_i in growth cones (7.12 $\pm$ 0.04) was not significantly different from pH_i measured at cell bodies (7.10 $\pm$ 0.04). ***e***, The application of cariporide (2 μM for 6 min, starting at 12.5 min) was accompanied by a reversible reduction in growth cone filopodia number and a reversible cessation of neurite outgrowth. Scale bar, 5 μm.

Rates of pH_i recovery from internal acid loads imposed by the NH_4^+ prepulse technique were used for the functional characterization of NHE1 mutants used in the present study (supplemental Figs. 1, 3, available at www.jneurosci.org as supplemental material) and to assess the effects of netrin-1, BDNF, and IGF-1 on Na^+/H^+ exchange activity (see Fig. 10), as described previously (Sheldon and Church, 2002). In the latter cases, two or more consecutive intracellular acid loads were imposed, the first one (or two) being used to calculate control rates of pH_i recovery for a given neuron and the second (or third) being performed under a test condition. Rates of pH_i recovery were determined by fitting the recovery portions of the pH_i records to a single-exponential function, and the first derivative of this function was used to determine the rate of pH_i change (dpH_i/dt). Instantaneous rates of pH_i recovery under control and test conditions were evaluated at 0.05 pH unit intervals of pH_i and compared statistically (Student's paired two-tailed *t* test) at corresponding values of pH_i.

Results

Inhibition of NHE1 activity reduces early neurite outgrowth in NGF-differentiated PC12 cells

Initially, we examined the role of NHE1 in early neurite outgrowth in NGF-differentiated PC12 cells, a well defined model system widely used in studies of neuritogenesis. These experiments [as well as those involving neocortical neurons (see below)] were performed under HCO_3^-/CO_2-buffered conditions to ensure the continued function of HCO_3^--dependent pH_i regulating mechanisms.

First, in the absence of published data, we confirmed by Western blot analysis that NHE1 is expressed in PC12 cells differentiated with NGF for 72 h (Fig. 1*a*). We then examined the effects of the specific Na^+/H^+ exchange inhibitor cariporide (Scholz et al., 1995), coapplied with NGF for 72 h at an NHE1-selective concentration (1 μM) (Masereel et al., 2003; Karmazyn et al., 2005) on early neurite formation, elongation, and elaboration. Compared with untreated (data not shown) or vehicle-treated (0.1% DMSO) (Fig. 1*b*,*c*) cells, 1 μM cariporide significantly reduced the total number and total cumulative length of neurites. Applied at 100 μM, to inhibit other plasmalemmal NHE isoforms, cariporide failed to exert additional inhibitory effects (Fig. 1*c*), further suggesting that the effect of 1 μM cariporide to reduce early neurite outgrowth in NGF-treated PC12 cells was consequent on the inhibition of NHE1.

The inhibitory effects of cariporide on early neurite outgrowth were reversible. As shown in Figure 1*d*, PC12 cells fixed after 24, 48, or 72 h treatment with NGF in the presence of 0.1% DMSO exhibited time-dependent increases in the formation and elongation of neurites. In parallel experiments, additional batches of PC12 cells were treated with 1 or 100 μM cariporide for 24 h, starting 24 h after the addition of NGF; cells were then either fixed 24 h after the addition of cariporide or cariporide-containing medium was washed off, and cells were incubated for an additional 24 h in cariporide-free medium before fixation (a total of 72 h in culture). Consistent with our initial observations, a 24 h exposure to 1 μM (data not shown) or 100 μM (Fig. 1*d*) cariporide significantly inhibited the neurite outgrowth that occurred between the 24 and 48 h time points in vehicle-treated PC12 cells.

However, cells that had been maintained in cariporide-free medium for an additional 24 h displayed a return to normal rates of growth, exhibiting total numbers and total cumulative lengths of neurites comparable with those observed in cells that had been cultured in the absence of cariporide for 48 h (Fig. 1*d*). Similar results were obtained in chick dorsal root ganglion explants, another well documented model system for the study of neurite outgrowth (data not shown).

Ion translocation and ERM binding are involved in NHE1 regulation of early neurite outgrowth in PC12 cells

As noted in Introduction, both the ion translocation and ERM binding/actin cytoskeletal anchoring functions of NHE1 are involved in the regulation of directed motility in non-neuronal cells. To assess whether these functions contribute to the regulation of early neurite morphogenesis by NHE1, NGF-differentiated PC12 cells were transiently transfected with cDNAs encoding full-length $NHE1_{HA}$ or mutant NHE1s deficient in either ion translocation ($NHE1–E266I_{HA}$) or ERM binding ($NHE1–KR/A_{HA}$) (Denker et al., 2000; Denker and Barber, 2002). In control experiments, NHE-deficient PS120 fibroblasts transfected with full-length $NHE1_{HA}$ or $NHE1\text{-}KR/A_{HA}$ exhibited cariporide-sensitive pH_i-dependent recoveries of pH_i from imposed internal acid loads, whereas untransfected cells and cells overexpressing $NHE1–E266I_{HA}$ did not (supplemental Fig. 1, available at www.jneurosci.org as supplemental material) (Denker et al., 2000).

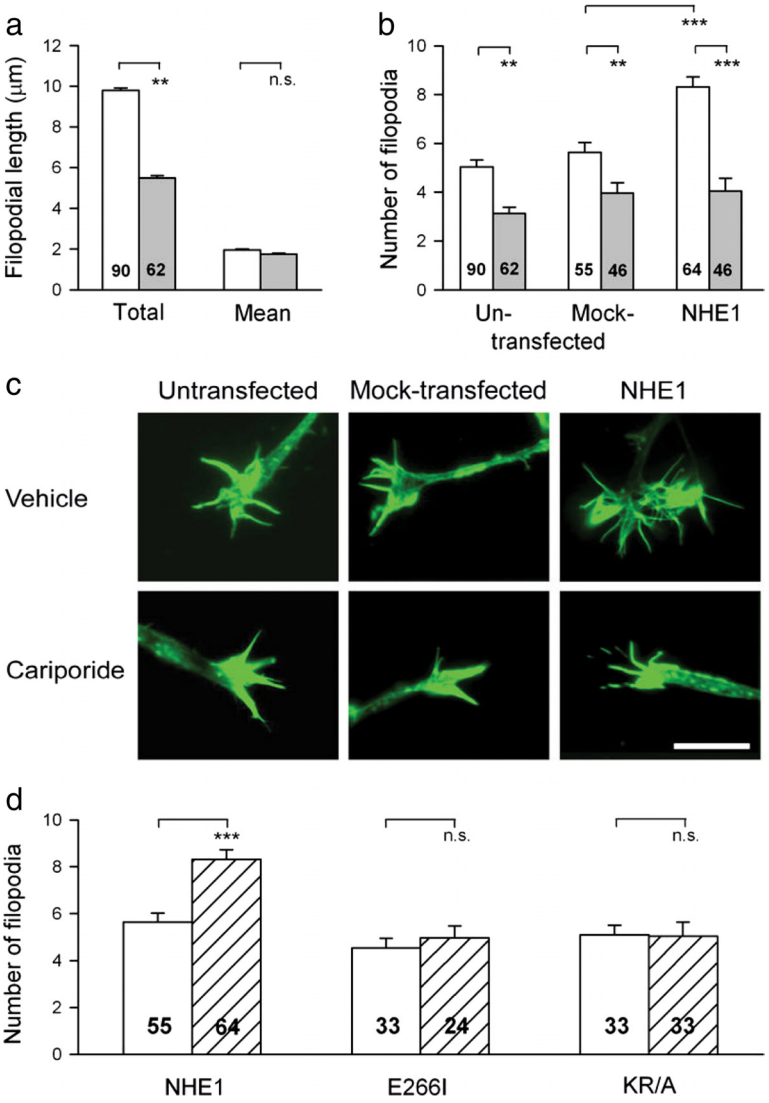

Figure 4. NHE1 regulates filopodia number in PC12 cell growth cones. PC12 cells were differentiated with 50 ng/ml NGF for 72 h. ***a***, Compared with vehicle-treated controls (white bars; 0.1% DMSO), 1 μM cariporide (gray bars) reduced the total length of filopodia per growth cone but not mean filopodial length. ***b***, Compared with untransfected cells cultured in the presence of cariporide vehicle (0.1% DMSO; white bars), 1 μM cariporide (gray bars) reduced the number of filopodia per growth cone. Conversely, compared with mock-transfected cells, overexpression of HA-tagged full-length NHE1 (NHE1) increased the number of growth cone filopodia in a cariporide-sensitive manner. ***c***, Representative images of growth cones under the experimental conditions quantified in ***b***. Cells stained with Alexa Fluor 488-conjugated phalloidin. Scale bar, 10 μm. ***d***, Compared with mock-transfected cells (white bars), overexpression of HA-tagged full-length NHE1, but not HA-tagged NHE1 mutants defective in either ion translocation (E266I) or ERM binding/actin cytoskeletal anchoring (KR/A) (hatched bars), increased the number of filopodia per growth cone. In ***a***, ***b***, and ***d***, error bars represent SEM, and *n* values (representing the number of growth cones examined under each experimental condition) are shown in the columns. $^{**}p < 0.01$; $^{***}p < 0.001$; n.s., not significant ($p > 0.05$).

PC12 cells transfected with full-length $NHE1_{HA}$ and subsequently differentiated with NGF for 72 h exhibited modest increases in the total number and total cumulative length of neurites, effects that were entirely sensitive to 1 μM cariporide (Fig. 2*a*,*b*). Quantification of the separate contributions of changes in the numbers and cumulative lengths of primary neurites and neurite branches to the changes in the total values indicated that the overexpression of full-length $NHE1_{HA}$ was especially associated with a marked increase in the cumulative length of branches (supplemental Fig. 2, available at www.jneurosci.org as supplemental material). In contrast, compared with untransfected cells, the overexpression of $NHE1–E266I_{HA}$ was associated with marked reductions in neurite formation and extension that were not further reduced by cariporide (Fig. 2*a*,*b*) (supplemental Fig. 2, available at www.jneurosci.org as supplemental material). Cells overexpressing $NHE1–KR/A_{HA}$ also exhibited reductions in neurite outgrowth that, in contrast to cells overexpressing $NHE1–E266I_{HA}$, were further reduced by 1 μM cariporide to levels comparable with those observed in cariporide-treated untransfected PC12 cells (Fig. 2*a*,*b*) (supplemental Fig. 2, available at www.jneurosci.org as supplemental material). The sensitivity to cariporide of the limited neurite outgrowth observed in PC12 cells overexpressing $NHE1–KR/A_{HA}$ presumably reflects the fact that this mutant supports cariporide-sensitive acid efflux. Similar results to those obtained in PC12 cells overexpressing $NHE1–KR/A_{HA}$ were obtained in cells overexpressing $NHE1–\Delta 556\text{-}564_{HA}$, a second NHE1 mutant with a disrupted ERM binding motif (supplemental Fig. 3, available at www.jneurosci.org as supplemental material).

Together, these results suggest that both ion translocation and ERM binding/actin cytoskeletal anchoring contribute to the regulation of early neurite morphogenesis by NHE1. The dominant-

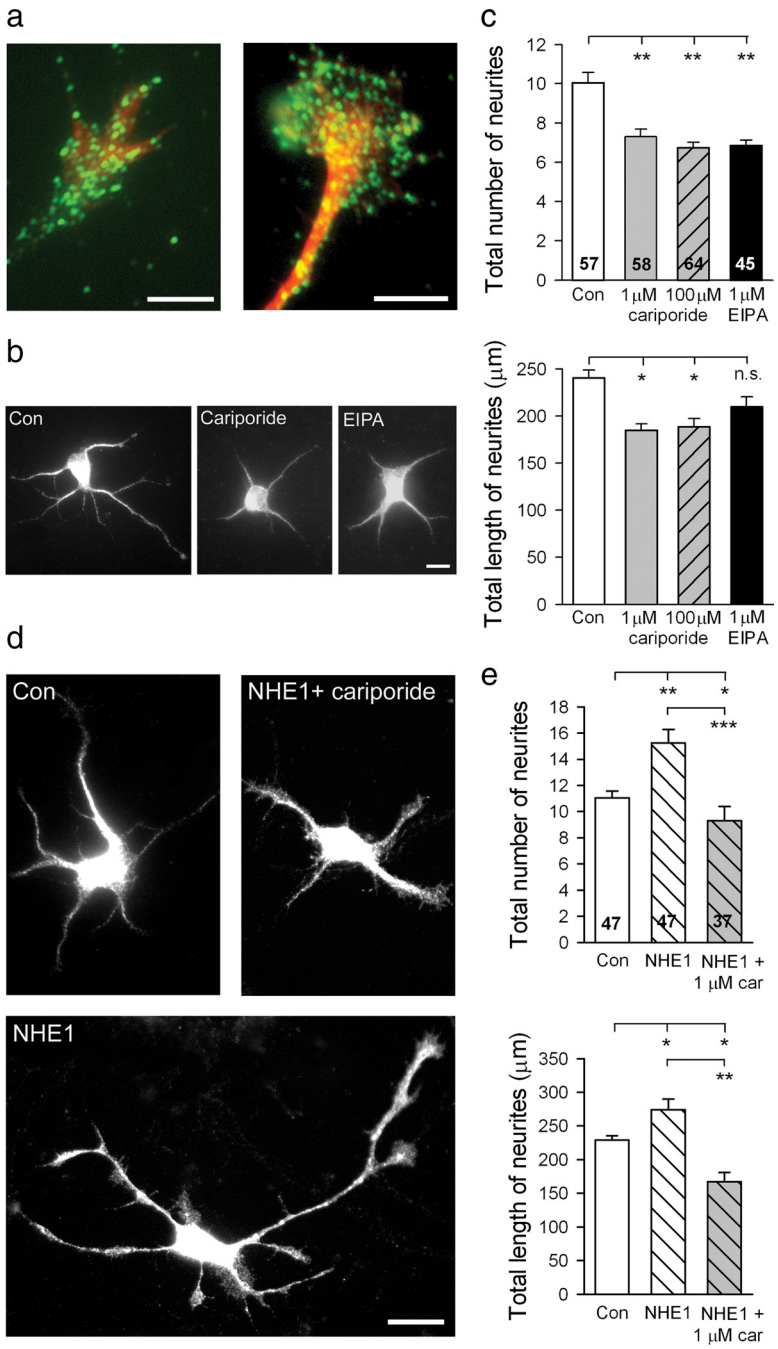

Figure 5. NHE1 regulates early neurite outgrowth in E16 WT mouse neocortical neurons. ***a***, Expression of endogenous NHE1 in growth cones from two different neurons at 3 div costained with anti-NHE1 antibody (green) and either Alexa Fluor 568-conjugated phalloidin (left) or anti-vinculin antibody (right). Scale bars, 5 μm. ***b***, Representative examples of neurons cultured for 72 h in the continuous presence of 0.1% DMSO (Con), 1 μM cariporide, or 1 μM EIPA. Neurons stained with anti-MAP2 antibody. Scale bar, 10 μm. ***c***, Quantification of the total number (top) and total cumulative length (bottom) of neurites per cell in neurons cultured for 72 h under control conditions (Con; 0.1% DMSO) or in the continuous presence of 1 μM cariporide, 100 μM cariporide, or 1 μM EIPA, as indicated on the figure. ***d***, Compared with untransfected neurons (Con), the overexpression of HA-tagged full-length NHE1 enhanced neurite outgrowth in a 1 μM cariporide-sensitive manner. Neurons were fixed at 3 div and labeled with anti-MAP2 antibody (untransfected cell) or anti-HA antibody (transfected cells). Scale bar, 20 μm. ***e***, Quantification of the total number (top) and total cumulative length (bottom) of neurites per cell in untransfected neurons (Con; white bars) and neurons transiently transfected with HA-tagged full-length NHE1 (NHE1), in the absence (white hatched bars) or presence (gray hatched bars) of 1 μM cariporide (car). In ***c*** and ***e***, experiments were conducted in parallel, all measured values are per cell, error bars represent SEM, and *n* values are shown in the columns. $^*p < 0.05$; $^{**}p < 0.01$; $^{***}p < 0.001$; n.s., not significant ($p > 0.05$). For ***c*** and ***e***, separated measurements of changes in the numbers and cumulative lengths of primary neurites per cell and neurite branches per cell to the total values shown are presented in supplemental Figures 4 and 5, respectively (available at www.jneurosci.org as supplemental material).

negative effects on neurite outgrowth observed after the overexpression of the ion translocation-deficient mutant NHE1–E266I$_{HA}$ or the ERM binding-deficient mutants NHE1–KR/A$_{HA}$ and NHE1–Δ556-564$_{HA}$ are in agreement with previous reports (Mitsui et al., 2005; Hisamitsu et al., 2006). As proposed by Hisamitsu et al. (2006), the dominant-negative effect of the ion translocation-deficient mutant may reflect the fact that the homodimerization of two active NHE1 subunits (and subsequent interaction between the monomers) is required for Na^+/H^+ exchange activity under physiological conditions, whereas the dominant-negative effects of the ERM binding-deficient mutants may reflect mislocalization and reduced levels of surface expression.

NHE1 is expressed and regulates pH_i and morphology in PC12 cell growth cones

Neurite growth is driven primarily by cytoskeletal rearrangements at the growth cone. Therefore, we examined whether NHE1 was expressed in PC12 cell growth cones, in which it would be well positioned to contribute to the regulation of neurite elaboration and/or elongation.

Endogenous NHE1 was observed as punctate staining at the soma, along developing neurites, and especially at the growth cone (Fig. 3*a*). To examine whether NHE1 was functional in the latter, spatially restricted compartment, we performed live-cell pH_i measurements in conjunction with DIC microscopy to monitor growth cone morphology and neurite extension. In agreement with a previous report (Dickens et al., 1989), we found that pH_i in the growth cones of actively extending neurites was consistently higher than in more proximal regions and also in the growth cones of non-extending neurites. Thus, in neurites that did not extend during the 30 min time course of a given experiment, growth cone pH_i (7.22 ± 0.03; $n = 10$) was not significantly different ($p = 0.58$) from that measured simultaneously in more proximal regions of primary neurites and/or at the soma (7.20 ± 0.02) (Fig. 3*b*). In contrast, pH_i in the growth cones of actively extending neurites (7.36 ± 0.02; $n = 10$) was significantly ($p < 0.01$) elevated compared with pH_i measured simultaneously in more proximal regions (7.23 ± 0.03) (Fig. 3*c*). Furthermore, cariporide reversibly reduced pH_i in the growth cones of actively extending neurites (Fig. 3*d*), an effect that was consistently accompanied by reversible reductions in growth cone filopodia

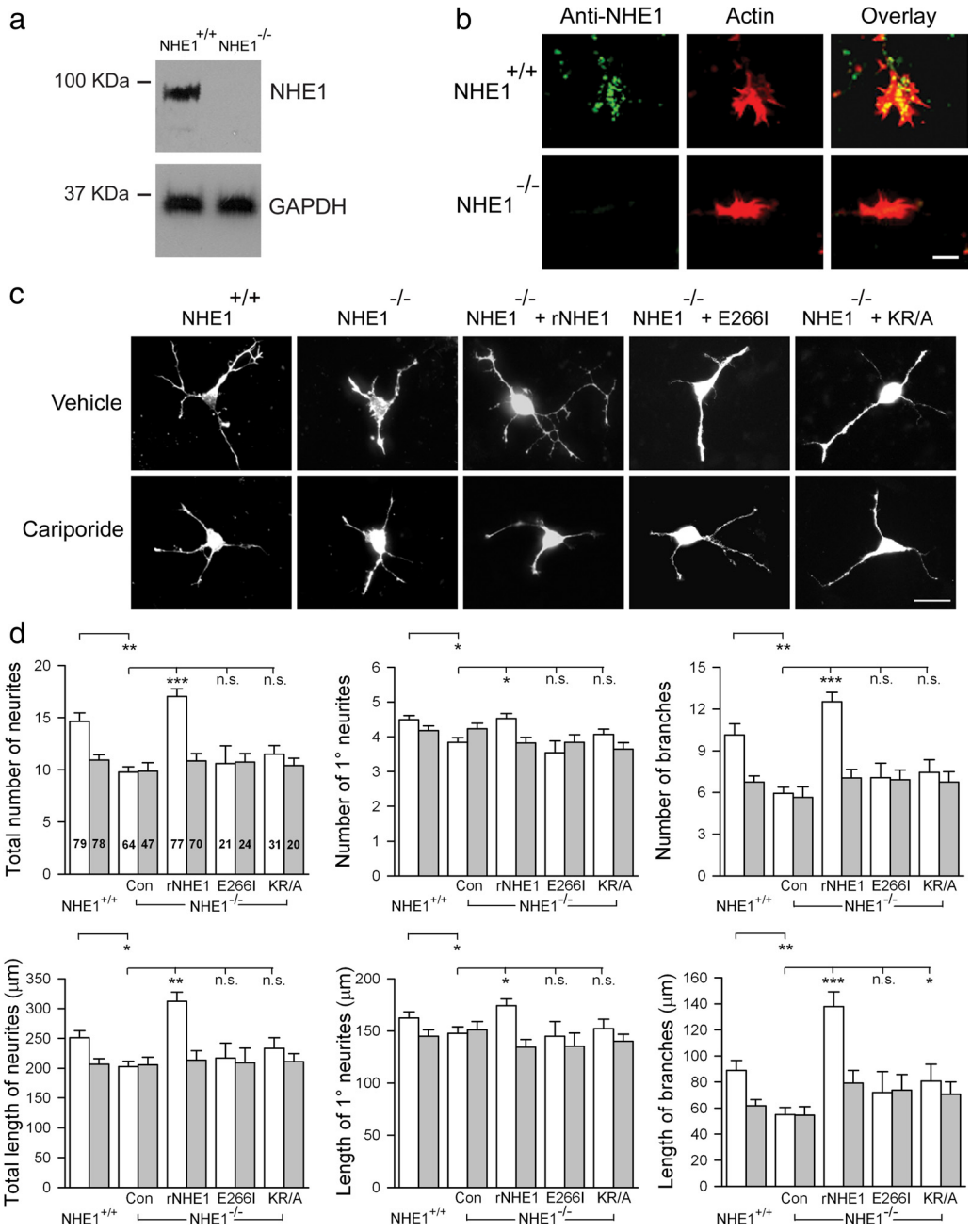

Figure 6. NHE1 and the regulation of early neurite outgrowth in P0.5 mouse neocortical neurons. ***a***, NHE1 was expressed in brain tissue from *NHE1*$^{+/+}$ but not *NHE1*$^{-/-}$ mice. Western blot analysis with anti-NHE1 antibody; GAPDH was used as a loading control. ***b***, Expression of endogenous NHE1 in growth cones of *NHE1*$^{+/+}$ and *NHE1*$^{-/-}$ neocortical neurons. Neurons fixed at 3 div and costained with anti-NHE1 antibody and Alexa Fluor 568-conjugated phalloidin. Scale bar, 5 μm. ***c***, Representative examples of morphologies of *NHE1*$^{+/+}$ neurons, *NHE1*$^{-/-}$ neurons, and *NHE1*$^{-/-}$ neurons transiently transfected with HA-tagged full-length recombinant NHE1 (*NHE1*$^{-/-}$ + rNHE1), NHE1-E266I (*NHE1*$^{-/-}$ + E266I), or NHE1-KR/A (*NHE1*$^{-/-}$ + KR/A) and cultured for 72 h in either the absence or presence of 1 μM cariporide. Untransfected and transfected neurons were stained with Alexa Fluor 568-conjugated phalloidin and anti-HA antibody, respectively. Scale bar, 20 μm. ***d***, Quantification of neurite outgrowth in neocortical neurons obtained from *NHE1*$^{+/+}$ and *NHE1*$^{-/-}$ littermates, in the absence (white bars) and presence (gray bars) of 1 μM cariporide. The reduced level of early neurite outgrowth observed in untransfected *NHE1*$^{-/-}$ neurons (Con) compared with *NHE1*$^{+/+}$ neurons was rescued by the overexpression of HA-tagged full-length NHE1 (rNHE1) but not NHE1–E266I (E266I) or NHE1–KR/A (KR/A). Experiments were conducted in parallel, all measured values are per cell, error bars represent SEM, and *n* values are shown in the columns. $*p < 0.05$; $**p < 0.01$; $***p < 0.001$; n.s., not significant ($p > 0.05$).

number and neurite extension (Fig. 3*e*). The detection of an NHE1-dependent elevated pH_i in the growth cones of actively extending neurites may have been facilitated by our use of a low concentration of BCECF (see Materials and Methods) and the relatively high level of NHE1 expression in this restricted compartment that, combined with geometric factors and the relatively low mobility of protons in cytoplasm, predisposes to the generation of subcellular pH_i heterogeneities via the activities of pH_i regulating mechanisms (Pantazis et al., 2006; Rojas et al., 2006; Vaughan-Jones et al., 2006).

To quantify the effects of NHE1 inhibition on growth cone filopodia number, PC12 cells were fixed and stained with phalloidin after differentiation with NGF for 72 h in the continuous presence of 1 μM cariporide. As shown in Figure 4*a*, cariporide led to a reduction in total but not mean filopodial length, indicating that the predominant effect was to reduce the number of

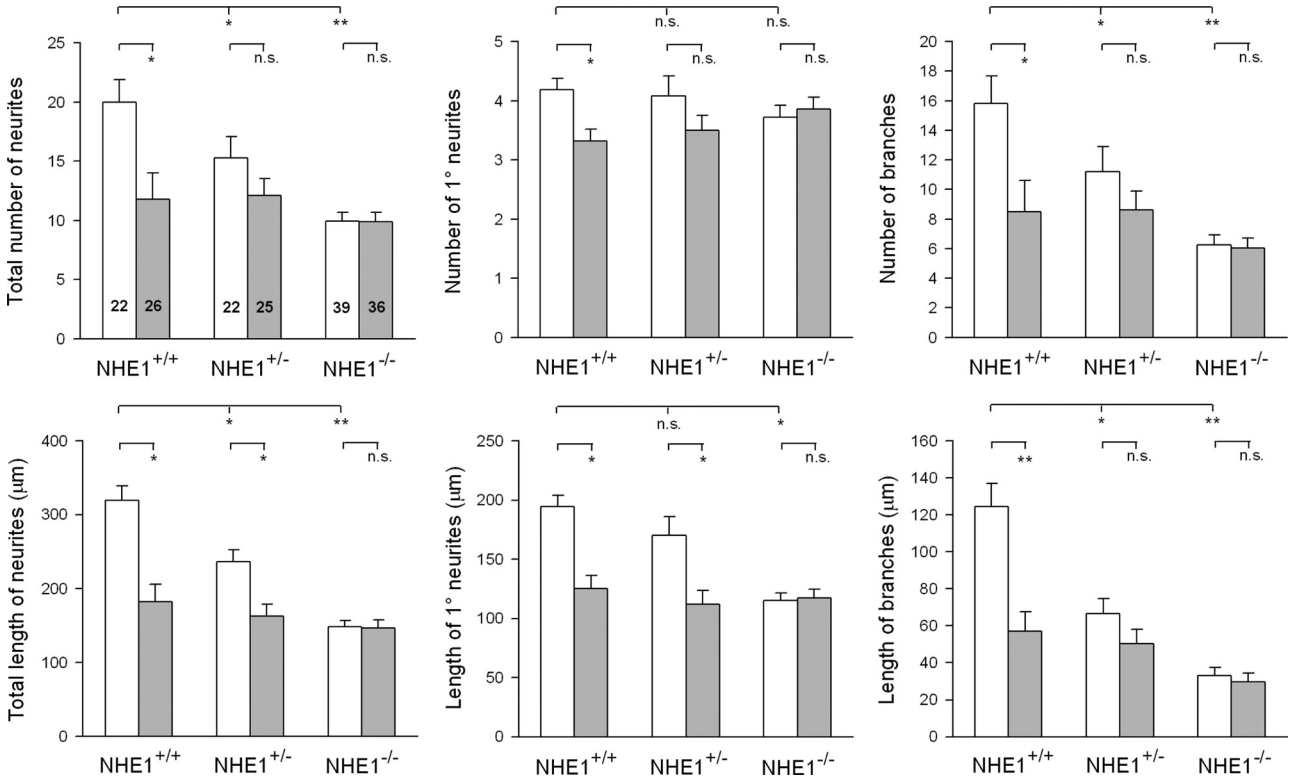

Figure 7. Early neurite outgrowth in *NHE1*$^{+/+}$, *NHE1*$^{+/-}$, and *NHE1*$^{-/-}$ neocortical neurons. Neurons obtained from P0.5 littermates were placed in primary culture for 72 h in the absence (white bars) or presence (gray bars) of 1 μM cariporide. Compared with *NHE1*$^{+/+}$ and *NHE1*$^{-/-}$ neurons, *NHE1*$^{+/-}$ neurons exhibited intermediate levels of early neurite outgrowth and sensitivity to 1 μM cariporide. Experiments were conducted in parallel, all measured values are per cell, error bars represent SEM, and *n* values are shown in the columns. *$p < 0.05$; **$p < 0.01$; n.s., not significant ($p > 0.05$).

growth cone filopodia. The effects of cariporide on growth cone filopodia number are quantified in Figure 4*b*, and representative examples of growth cone morphologies observed in the absence and presence of cariporide are presented in Figure 4*c*. As also shown in Figure 4, *b* and *c*, overexpression of full-length $NHE1_{HA}$ increased the number of filopodia in PC12 cell growth cones in a cariporide-sensitive manner. In contrast, overexpression of either NHE1–$E266I_{HA}$ or NHE1–KR/A_{HA} failed to increase growth cone filopodia number (Fig. 4*d*).

NHE1 regulates early neurite outgrowth in E16 wild-type mouse neocortical neurons

The above findings indicate that NHE1 contributes to the regulation of early neurite morphogenesis in the NGF-differentiated PC12 cell model system. To confirm these initial findings, selected experiments were repeated in neocortical neurons isolated from E16 WT mice and maintained in primary culture for 72 h.

Consistent with findings in NGF-differentiated PC12 cells, NHE1 was expressed in the growth cones of WT neocortical neurons (Fig. 5*a*). As in PC12 cells, 1 μM cariporide reduced the total number and cumulative length of neurites, and 100 μM cariporide failed to exert additional inhibitory effects (Fig. 5*b*, *c*). Results similar to those observed with 1 μM cariporide were obtained with 1 μM EIPA, another potent inhibitor of Na^+/H^+ exchange activity that, like cariporide, leads to pseudopodial retraction and the inhibition of motility in non-neuronal cells (Lagana et al., 2000) (Fig. 5*b*, *c*). Quantification of the separate contributions of changes in the numbers and cumulative lengths of primary neurites and neurite branches to the changes in the total values indicated that the NHE inhibitors exerted more marked effects on neurite branches than on primary neurites (supplemental Fig. 4, available at www.jneurosci.org as supplemental material). The effects of cariporide and EIPA on early neurite outgrowth in E16 WT neocortical neurons were entirely reversible and were not associated with the induction of necrosis or apoptosis, as assessed by lactate dehydrogenase release and TUNEL staining, respectively (data not shown). Finally, the total number and cumulative length of neurites were increased in E16 WT neocortical neurons overexpressing full-length $NHE1_{HA}$, effects that were blocked by 1 μM cariporide (Fig. 5*d*, *e*) and that primarily reflected increases in the number and cumulative length of second- and higher-order branches (supplemental Fig. 5, available at www.jneurosci.org as supplemental material).

Early neurite outgrowth is reduced in *NHE1*$^{-/-}$ neocortical neurons

To extend the aforementioned findings, which were obtained using a predominantly pharmacological approach, we next examined the role of NHE1 in early neurite outgrowth in cultured (3 div) neocortical neurons obtained from P0.5 *Nhe1* homozygous mutant (*NHE1*$^{-/-}$) mice and their heterozygous (*NHE1*$^{+/-}$) and/or WT (*NHE1*$^{+/+}$) littermates.

Initially, we confirmed by Western blot analysis using anti-NHE1 antibody that NHE1 protein was absent in brain tissue from *NHE1*$^{-/-}$ mice (Fig. 6*a*) and determined that NHE1 was endogenously expressed at the growth cones of neocortical neurons obtained from P0.5 *NHE1*$^{+/+}$ but not P0.5 *NHE1*$^{-/-}$ mice (Fig. 6*b*). As illustrated in Figure 6*c* and quantified in Figure 6*d*, neurons isolated from *NHE1*$^{-/-}$ mice possessed fewer and shorter neurites, especially branches, than neurons isolated from

their *NHE1*$^{+/+}$ littermates. As expected, 1 μM cariporide failed to exert additional inhibitory effects in *NHE1*$^{-/-}$ neurons ($p > 0.05$ for all parameters measured) (Fig. 6*c*, *d*). Intermediate levels of neurite outgrowth and sensitivity to cariporide were observed in neocortical neurons obtained from P0.5 heterozygous (*NHE1*$^{+/-}$) littermates (Fig. 7), further suggesting a correlation between neurite outgrowth and NHE1 protein levels. Finally, the introduction of exogenous full-length $NHE1_{HA}$, but not NHE1 mutants deficient in either ion translocation activity (NHE1–$E266I_{HA}$) or ERM binding/actin cytoskeletal anchoring (NHE1–KR/A_{HA}), into *NHE1*$^{-/-}$ neurons resulted in significant increases in the numbers and cumulative lengths of neurites, especially branches, that in turn were inhibited by 1 μM cariporide (Fig. 6*c*, *d*).

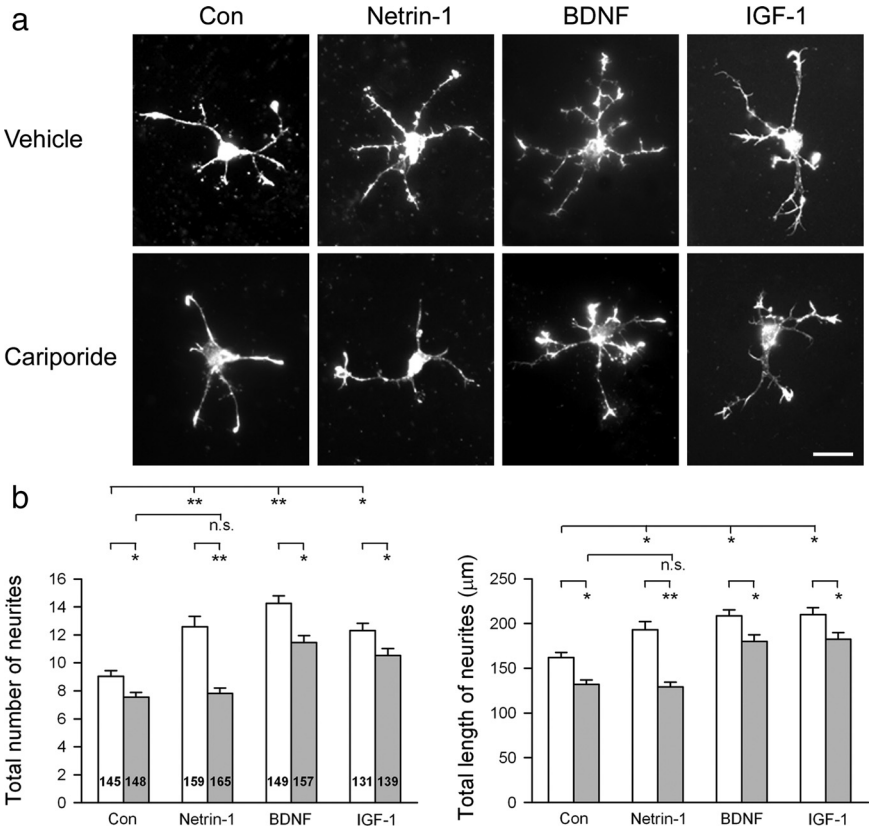

Figure 8. Effects of cariporide on increases in early neurite outgrowth induced by netrin-1, BDNF, and IGF-1 in P0.5 *NHE1*$^{+/+}$ neocortical neurons. ***a***, Representative examples of *NHE1*$^{+/+}$ neurons cultured in the absence (Con) or presence of 100 ng/ml netrin-1, 50 ng/ml BDNF, or 50 ng/ml IGF-1 for 72 h, in the continuous presence of either cariporide vehicle (0.1% DMSO) or 1 μM cariporide. Neurons fixed at 3 div and stained with Alexa Fluor 568-conjugated phalloidin. Scale bar, 20 μm. ***b***, Quantification of the total number (left) and total cumulative length (right) of neurites per cell in *NHE1*$^{+/+}$ neocortical neurons under the conditions shown on the figure, in the absence (white bars) and presence (gray bars) of 1 μM cariporide. Experiments were conducted in parallel, all measured values are per cell, error bars represent SEM, and *n* values are shown in the columns. *$p < 0.05$; **$p < 0.01$; n.s., not significant ($p > 0.05$). The separated measurements of changes in the numbers and cumulative lengths of primary neurites per cell and neurite branches per cell to the total values shown in ***b*** are presented in supplemental Figure 6 (available at www.jneurosci.org as supplemental material).

The role of NHE1 in trophic factor-stimulated early neurite outgrowth

The preceding results identify a role for NHE1 in the regulation of early neurite morphogenesis in mouse neocortical neurons under basal (i.e., nonstimulated) conditions. However, the size and shape of neuritic arbors are influenced by environmental factors. Therefore, we examined whether NHE1 might also influence the effects of three agents that are known to promote neurite elongation and/or branching in mammalian central neurons, i.e., netrin-1 (Barallobre et al., 2005; Round and Stein, 2007), BDNF (Huang and Reichardt, 2001), and IGF-1 (Niblock et al., 2000). These experiments were performed on neocortical neurons obtained from P0.5 *NHE1*$^{+/+}$ mice and their NHE1-null mutant (*NHE1*$^{-/-}$) littermates and maintained in primary culture for 72 h.

As expected, 100 ng/ml netrin-1, 50 ng/ml BDNF, and 50 ng/ml IGF-1 each enhanced early neurite elaboration and extension in *NHE1*$^{+/+}$ neurons (Fig. 8*a*, *b*). In the cases of BDNF- and IGF-1-treated neurons, 1 μM cariporide exerted relatively modest inhibitory effects on the total number and cumulative length of neurites (Fig. 8*a*, *b*) that primarily reflected reductions in the number and cumulative length of neurite branches rather than primary neurites (supplemental Fig. 6, available at www.jneurosci.org as supplemental material). In contrast, 1 μM cariporide eff-

ectively abolished the early neurite outgrowth-promoting effects of netrin-1; for all parameters measured, there were no significant differences between results obtained in cariporide-treated *NHE1*$^{+/+}$ neurons cultured in the presence versus the absence of netrin-1 (Fig. 8*a*, *b*) (supplemental Fig. 6, available at www.jneurosci.org as supplemental material). Similar results with netrin-1, BDNF, and IGF-1 were obtained in neocortical neurons isolated from E16 WT mice (data not shown).

We also examined whether cariporide affected the rapid changes in growth cone morphology which are known to occur during acute exposure to netrin-1. Consistent with previous reports in neocortical neurons (Dent et al., 2004) (see also Shekarabi and Kennedy, 2002; Shekarabi et al., 2005), exposure of *NHE1*$^{+/+}$ neurons to netrin-1 for 10 or 30 min caused significant increases in the number of growth cone filopodia that, in turn, were markedly attenuated by the concomitant application of 1 μM cariporide (Fig. 9*a–c*). Reminiscent of findings in PC12 cells (Fig. 4), the number of growth cone filopodia observed under control conditions (i.e., in the absence of exogenously added netrin-1) was also significantly reduced by the acute application of 1 μM cariporide (Fig. 9*a–c*).

As noted in Introduction, a large number of external agents are known to regulate the ion translocation activity of NHE1, raising the possibility that the marked sensitivity to cariporide of the growth-promoting effects of netrin-1 (compare BDNF and IGF-1) could be consequent on the differential activation of NHE1 by netrin-1. Therefore, we examined the effects of netrin-1, BDNF, and IGF-1 on steady-state pH_i and Na^+/H^+ exchange activity in P0.5 WT (*NHE1*$^{+/+}$) neocortical neurons. As illustrated in Figure 10*a*, netrin-1 failed to affect steady-state pH_i at the growth cone, which in turn was reversibly reduced by 1 μM cariporide (see also Fig. 3*d*). Examined at the level of the cell body, netrin-1 also failed to affect both steady-state pH_i and the cariporide-sensitive recovery of pH_i from imposed intracellular

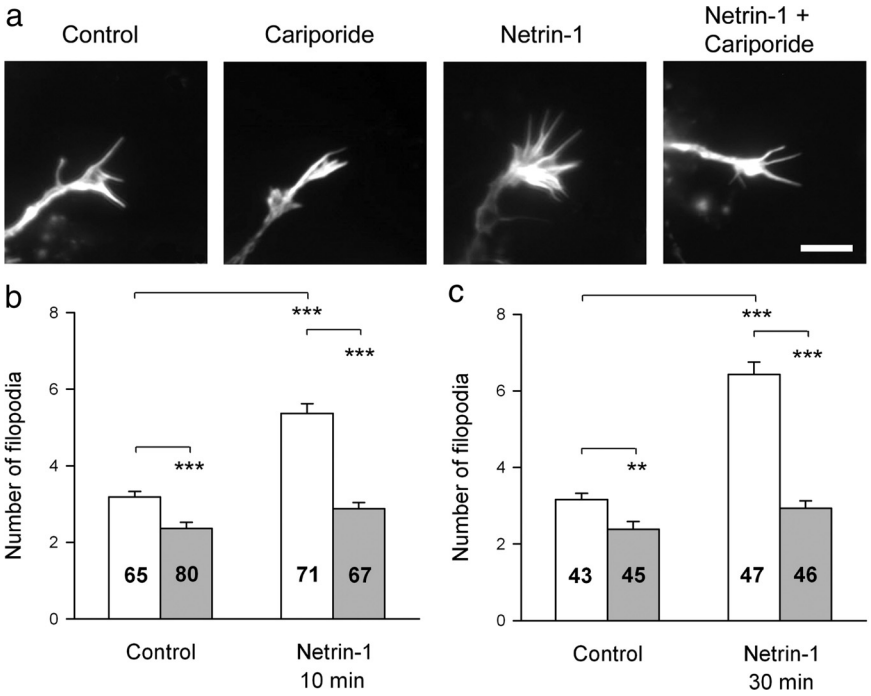

Figure 9. Cariporide attenuates netrin-1-induced increases in growth cone filopodia number in *NHE1*$^{+/+}$ neocortical neurons. ***a***, Representative examples of *NHE1*$^{+/+}$ neurons (3 div) exposed to cariporide vehicle (Control; 0.1% DMSO) or 100 ng/ml netrin-1 for 10 min, in the absence or presence of 1 μM cariporide, as indicated in the figure. Neurons stained with Alexa Fluor 488-conjugated phalloidin. Scale bar, 5 μm. ***b***, ***c***, Quantification of growth cone filopodia number in *NHE1*$^{+/+}$ neurons exposed for 10 (***b***) or 30 min (***c***) to cariporide vehicle (0.1% DMSO; white bars) or 1 μM cariporide (gray bars) in the absence (Control) or presence of 100 ng/ml netrin-1, as indicated in the figure. Compared with vehicle-treated controls, netrin-1 increased the number of growth cone filopodia per growth cone. Cariporide at 1 μM reduced both the number of growth cone filopodia per growth cone under control conditions (see also Fig. 4) and the increases in growth cone filopodia number per growth cone elicited by netrin-1. In ***b*** and ***c***, error bars represent SEM, and *n* values (representing the number of growth cones examined under each experimental condition) are shown in the columns. $^{**}p < 0.01$; $^{***}p < 0.001$.

acid loads (Fig. 10*b*) (we were unable to conduct the latter experiments in growth cones because the acute imposition of internal acid loads led to their collapse). To formally assess the effects of netrin-1, BDNF, and IGF-1 on NHE1 activity, we compared rates of pH_i recovery from internal acid loads imposed before and after 10–45 min pretreatment with each of the agents. As illustrated in Figure 10*c–e*, netrin-1, BDNF, and IGF-1 each failed to significantly affect rates of pH_i recovery at all absolute values of pH_i examined. In separate experiments, we confirmed that none of the agents tested affected intrinsic intracellular buffering power or background acid loading rates (data not shown). Together, these results indicate that activation of NHE1 is unlikely to underlie the cariporide-sensitive growth-promoting effects of netrin-1 in WT neocortical neurons.

In the final series of experiments, we examined the effects of netrin-1, BDNF, and IGF-1 on neurite outgrowth in *NHE1*$^{-/-}$ neurons. In agreement with the limited sensitivity to cariporide of BDNF- and IGF-1-induced increases in neurite outgrowth in *NHE1*$^{+/+}$ neurons, the growth-promoting effects of BDNF and IGF-1 were maintained in *NHE1*$^{-/-}$ neurons (Fig. 11*a*, *b*). In contrast, but entirely consistent with the marked sensitivity to cariporide of netrin-1-induced increases in neurite outgrowth in *NHE1*$^{+/+}$ neurons, netrin-1 failed to promote early neurite elaboration or elongation in *NHE1*$^{-/-}$ neurons (Fig. 11*a*, *b*). Quantification of the separate contributions of changes in the numbers and cumulative lengths of primary neurites and neurite branches to the changes in the total values illustrated in Figure 11*b* are provided in supplemental Figure 7 (available at www.jneurosci.org as supplemental material). Finally, as illustrated in Figure 12, the failure of netrin-1 to promote early neurite outgrowth in *NHE1*$^{-/-}$ neurons was rescued in *NHE1*$^{-/-}$ neurons overexpressing full-length $NHE1_{HA}$ but not the ion translocation-deficient mutant NHE1–$E266I_{HA}$. Cariporide (1 μM) inhibited the growth-promoting effects of netrin-1 in *NHE1*$^{-/-}$ neurons transfected with full-length $NHE1_{HA}$ but exerted no effect on the residual outgrowth observed in *NHE1*$^{-/-}$ neurons transfected with NHE1–$E266I_{HA}$. Quantification of the separate contributions of changes in the numbers and cumulative lengths of primary neurites and neurite branches to the changes in the total values shown in Figure 12 are presented in supplemental Figure 8 (available at www.jneurosci.org as supplemental material) and indicate that, as in *NHE1*$^{+/+}$ neurons (Fig. 8) (supplemental Fig. 6, available at www.jneurosci.org as supplemental material), the growth-promoting effects of netrin-1 in *NHE1*$^{-/-}$ neurons transfected with full-length $NHE1_{HA}$ primarily reflected increases in the number and cumulative length of branches rather than primary neurites.

Together, these results indicate that ion translocation mediated by NHE1 is not a direct downstream target of netrin-1; rather, they are consistent with the possibility that the pH_i environment provided by NHE1 activity is an important factor in netrin-1 signaling to promote early neurite outgrowth.

Discussion

Cytoskeletal anchoring stabilizes ion transport proteins in specific membrane domains and localizes their activities in the proximity of signaling pathways to regulate cytoskeletal dynamics. In the case of NHE1, this plasma membrane-resident isoform accumulates at the leading edge of non-neuronal cells in which its activity regulates polarized membrane protrusion and directional motility. The results presented here support an analogous role for NHE1 in the regulation of early neurite outgrowth and identify a previously unrecognized role for NHE1 in the promotion of early neurite morphogenesis by netrin-1.

A number of mechanisms have been proposed to subserve the effects of NHE1 on leading edge membrane protrusion in non-neuronal cells (Cardone et al., 2005; Meima et al., 2007; Stock et al., 2008), and similar mechanisms could contribute to the regulation of early neurite morphogenesis described here. First, H^+ translocation at the growth cone could promote the formation of subplasmalemmal alkaline and/or extracellular acidic microdomains to regulate, respectively, actin cytoskeletal dynamics and the strength of the cell-substrate adhesions required to support neurite outgrowth. Na^+/H^+ exchange also promotes Na^+ and, via reverse Na^+/Ca^{2+} exchange, Ca^{2+} influx (Sheldon et al., 2004; Luo et al., 2005), with additional potential effects on neurite outgrowth (Brackenbury et al., 2008). Second, functioning in parallel with other ion transporters, NHE1 could promote a net gain of NaCl and water entry, leading to localized swelling at the

growth cone that could supply sufficient force to drive membrane protrusion. Third, acting as a scaffold, NHE1 could not only recruit ERM (Denker et al., 2000; Wu et al., 2004) and other actin-regulatory proteins (Aharonovitz et al., 2000; Xue et al., 2007) to the growth cone plasma membrane but also localize them in the proximity of NHE1-dependent $[ion]_i$ microdomains to modulate their activities. Although additional experiments are required to confirm or refute many of these possibilities, results presented here support the notion that NHE1 regulates early neurite morphogenesis at least in part by providing an elevated pH_i at the growth cone. Thus, pH_i in the growth cones of actively extending neurites was consistently higher than in more proximal regions or in the growth cones of non-extending neurites, and cariporide-induced reductions in pH_i in the growth cones of actively extending neurites were associated with reductions in growth cone filopodia number. A role for pH_i is also suggested by the facts that NHE1-null neurons exhibit a lower resting pH_i (Yao et al., 1999) and reduced neurite elaboration and elongation (present study) than their WT counterparts, with *NHE1*$^{+/-}$ neurons exhibiting intermediate levels of NHE1-dependent H^+ extrusion (Luo et al., 2005) and neurite outgrowth. NHE1-dependent elevations in growth cone pH_i could affect actin cytoskeletal remodeling by altering the state of actin polymerization directly and/or by modulating the activities of actin-binding and other proteins that together regulate the dynamic reorganization of the actin cytoskeleton (Srivastava et al., 2007, 2008). For example, increases in pH_i promote not only the activation of actin depolymerizing factor and cofilin, which enhance filopodial dynamics and neurite outgrowth, but also their translocation to the leading edge of migrating cells (Bernstein et al., 2000; Frantz et al., 2008). In addition, H^+ efflux by NHE1 promotes the activation of Cdc42 (Frantz et al., 2007), a finding of particular interest given the importance of this Rho-family GTPase for promoting filopodia formation and neurite outgrowth (da Silva and Dotti, 2002; Govek et al., 2005; Heasman and Ridley, 2008) (see below).

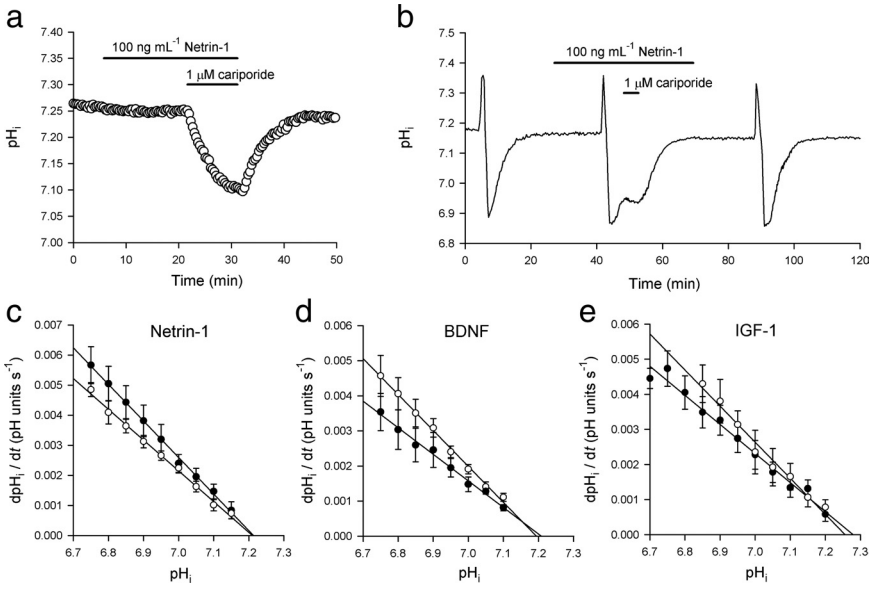

Figure 10. Effects of netrin-1, BDNF, and IGF-1 on pH_i in *NHE1*$^{+/+}$ mouse neocortical neurons. ***a***, Netrin-1 (100 ng/ml) failed to affect steady-state pH_i at the growth cones of actively extending neurites, whereas 1 μM cariporide caused a reversible reduction. The record is the mean of data obtained from two growth cones recorded simultaneously on the same coverslip and is representative of six independent experiments (a total of 9 growth cones). ***b***, Internal acid loads were imposed by the NH_4^+-prepulse technique before, during, and after the application of 100 ng/ml netrin-1. Netrin-1 failed to affect steady-state pH_i or pH_i recovery from an imposed acid load, which in turn was blocked by 1 μM cariporide. The record is the mean of data obtained from five neuronal cell bodies recorded simultaneously on the same coverslip and is representative of six independent experiments (a total of 44 neurons). ***c–e***, Plots of the pH_i dependencies of the rates of pH_i recovery from internal acid loads before (black circles) and after (white circles) pretreatment with 100 ng/ml netrin-1 (***c***), 50 ng/ml BDNF (***d***), or 50 ng/ml IGF-1 (***e***). Rates of pH_i recovery were evaluated at 0.05 unit intervals of pH_i, and errors bars ($n \geq 5$ independent measurements for all data points) represent SEM. At all absolute values of pH_i, there were no significant differences between rates of pH_i recovery measured before or during exposure to a test agent. Continuous lines represent the weighted nonlinear regression fits to the data points indicated for each experimental condition.

The observation that neurite outgrowth is able to proceed, albeit at a reduced rate, in *NHE1*$^{-/-}$ neurons suggests that NHE1 plays a permissive or facilitatory rather than determinant role in regulating early neurite morphogenesis under basal conditions. Similarly, although NHE1 is required for maximally efficient cell migration in non-neuronal cells, it is not essential for the development of the migratory response (Hayashi et al., 2008). The fact that NHE1-null mice, although exhibiting a distinctive neurological phenotype that includes ataxia, truncal instability, seizures, and selective neuronal death, do not display gross neurodevelopmental defects (Cox et al., 1997; Bell et al., 1999) also points to a permissive role for NHE1 in neurite morphogenesis, although it must be noted that interpretation of the *NHE1*$^{-/-}$ phenotype is complicated by alterations in the expression and/or activities of other pH_i regulating mechanisms and Na^+ influx pathways in *NHE1*$^{-/-}$ neurons that compensate for the loss of NHE1 (Xia et al., 2003; Xue et al., 2003; Schwab et al., 2005) (see also Putney and Barber, 2004; Zhou et al., 2004). Similarly, mice lacking the Cl^-/HCO_3^- exchanger AE3 (Hentschke et al., 2006), the Na^+–K^+–$2Cl^-$ cotransporter NKCC1 (Flagella et al., 1999), or the K^+–Cl^- cotransporter KCC2 (Hübner et al., 2001) do not exhibit gross histological abnormalities, despite the fact that these transport mechanisms are also known to regulate neurite outgrowth (Nakajima et al., 2007; Pieraut et al., 2007; Blaesse et al., 2009). Although NHE1 does not appear to be essential for early neurite outgrowth under basal conditions, a permissive role is not without potential consequences. In particular, as noted in Introduction, an important characteristic of NHE1 is that its activity is regulated by changes in extracellular pH (as caused, for example, by inflammation or injury) and also a large number of environmental stimuli that act via a variety of membrane receptors (e.g., G-protein-coupled receptors, receptor tyrosine kinases, and integrins) coupled to diverse signaling networks (Orlowski and Grinstein, 2004; Vaughan-Jones et al., 2009). Many of these factors also affect the outgrowth of neurites, placing NHE1 in a potential position to act as an integrator of multiple external cues and intracellular effector mechanisms that together regulate neurite morphogenesis.

Consistent with a permissive role for NHE1 in regulating early neurite morphogenesis, NHE1 exerted only modest effects on the growth-promoting actions of BDNF and IGF-1. In striking contrast, however, the promotion of early neurite morphogenesis by netrin-1 was markedly inhibited by reductions in NHE1 expression and activity. Interestingly, netrin-1 acting through the deleted in colorectal cancer (DCC) receptor leads to increases in growth cone filopodia number, neurite branching, and neurite

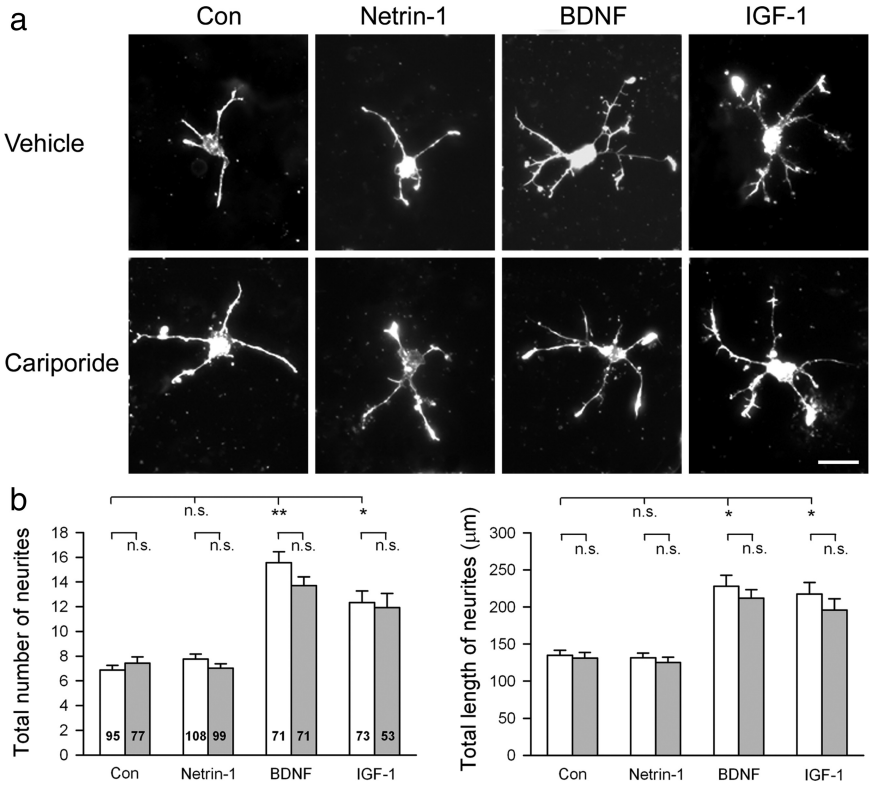

Figure 11. Netrin-1 fails to enhance early neurite outgrowth in *NHE1*$^{-/-}$ neocortical neurons. ***a***, Representative examples of *NHE1*$^{-/-}$ neurons cultured in the absence (Con) or presence of 100 ng/ml netrin-1, 50 ng/ml BDNF, or 50 ng/ml IGF-1, in the presence of either cariporide vehicle (0.1% DMSO) or 1 μM cariporide. Neurons fixed at 3 div and stained with Alexa Fluor 568-conjugated phalloidin. Scale bar, 20 μm. ***b***, Quantification of early neurite outgrowth in *NHE1*$^{-/-}$ neocortical neurons under the conditions shown in the figure, in the absence (white bars) and presence (gray bars) of 1 μM cariporide. Experiments were conducted in parallel, all measured values are per cell, error bars represent SEM, and *n* values are shown in the columns. *$p < 0.05$; **$p < 0.01$; n.s., not significant ($p > 0.05$). The separated measurements of changes in the numbers and cumulative lengths of primary neurites per cell and neurite branches per cell to the total values shown in ***b*** are presented in supplemental Figure 7 (available at www.jneurosci.org as supplemental material).

extension (Li et al., 2002; Shekarabi and Kennedy, 2002; Dent et al., 2004; Shekarabi et al., 2005; Tang and Kalil, 2005), which are the same features of neurite morphogenesis that are particularly sensitive to regulation by NHE1. [We have confirmed that DCC is expressed at the growth cones of our preparation of WT mouse neocortical neurons and that a function-blocking antibody to DCC (Keino-Masu et al., 1996) abolishes netrin-1-induced neurite outgrowth in these cells (D. M. Moniz, W.-C. Sin, and J. Church, unpublished findings).] Together, these observations point to NHE1 as an important factor in the stimulation of early neurite morphogenesis by netrin-1/DCC. In this regard, a number of admittedly speculative possibilities exist.

For example, NHE-dependent changes in pH_i have found been recently to control the surface recruitment of Dishevelled by Frizzled and thereby regulate Wnt signaling (Simons et al., 2009), raising the intriguing possibility that growth cone pH_i regulation by NHE1 might affect the recruitment of Cdc42, Rac1, Pak1, and N-WASP (neuronal Wiskott-Aldrich syndrome protein) into the intracellular signaling complex that promotes growth cone expansion in response to netrin-1 binding to DCC (Shekarabi et al., 2005). In addition, Cdc42 plays a key role in the promotion of neurite outgrowth by netrin-1/DCC (Barallobre et al., 2005; Govek et al., 2005; Round and Stein, 2007), and the finding that H^+ efflux by NHE1 promotes the activation of Cdc42 at the leading edge of migrating fibroblasts (see above) provides another plausible explanation for the regulation of netrin-1-stimulated neurite outgrowth by NHE1. Ion translocation by NHE1 could also affect the elevations in growth cone $[Ca^{2+}]_i$ (Tang and Kalil, 2005; Wang and Poo, 2005) and/or $[cAMP]_i$ (Ming et al., 1997) that also play important roles in netrin-1/DCC signaling in some cell types. Thus, not only do changes in extracellular and intracellular pH modulate the activities of many Ca^{2+}-permeable ion channels and the release of Ca^{2+} from intracellular stores (Tombaugh and Somjen, 1998; Traynelis, 1998; Willoughby et al., 2001; Huang et al., 2008) but also the catalytic activities of Ca^{2+}-stimulable transmembrane adenylyl cyclases are regulated directly by physiologically relevant changes in pH_i (Litvin et al., 2003; Willoughby et al., 2005). Finally, netrin-1 may regulate adhesive complexes to promote neurite outgrowth (Li et al., 2004; Liu et al., 2004; Ren et al., 2004). Although NHE1 may not be structurally associated with adhesion molecules, it's activity promotes the proper assembly and turnover of focal adhesion complexes at the leading edge of migrating cells (Meima et al., 2007; Srivastava et al., 2008), in which NHE1-dependent H^+ efflux also facilitates adhesion to the extracellular matrix (Stock et al., 2008). Together, these observations provide another possible link between NHE1 and the stimulation of early neurite morphogenesis by netrin-1.

Netrin-1 is a potential therapeutic target for nerve regeneration in degenerative diseases and after injury and also affects a wide range of processes in non-neuronal cells, including adhesion, morphogenesis, migration, and survival (Baker et al., 2006; Cirulli and Yebra, 2007). In light of the present findings, it will be interesting to determine whether NHE1 also regulates the effects of netrin-1 on regenerative neurite sprouting *in vivo* and in non-neuronal tissues.

References

Aharonovitz O, Zaun HC, Balla T, York JD, Orlowski J, Grinstein S (2000) Intracellular pH regulation by Na^+/H^+ exchange requires phosphatidylinositol 4,5-bisphosphate. J Cell Biol 150:213–224.

Arimura N, Kaibuchi K (2007) Neuronal polarity: from extracellular signals to intracellular mechanisms. Nat Rev Neurosci 8:194–205.

Baker KA, Moore SW, Jarjour AA, Kennedy TE (2006) When a diffusible axon guidance cue stops diffusing: roles for netrins in adhesion and morphogenesis. Curr Opin Neurobiol 16:529–534.

Barallobre MJ, Pascual M, Del Río JA, Soriano E (2005) The Netrin family of guidance factors: emphasis on Netrin-1 signalling. Brain Res Rev 49:22–47.

Bell SM, Schreiner CM, Schultheis PJ, Miller ML, Evans RL, Vorhees CV, Shull GE, Scott WJ (1999) Targeted disruption of the murine *Nhe1* locus induces ataxia, growth retardation and seizures. Am J Physiol 276:C788–C795.

Bernstein BW, Painter WB, Chen H, Minamide LS, Abe H, Bamburg JR (2000) Intracellular pH modulation of ADF/cofilin proteins. Cell Motil Cytoskeleton 47:319–336.

Blaesse P, Airaksinen MS, Rivera C, Kaila K (2009) Cation-chloride cotransporters and neuronal function. Neuron 61:820–838.

Brackenbury WJ, Djamgoz MB, Isom LL (2008) An emerging role for voltage-gated Na^+ channels in cellular migration: regulation of central

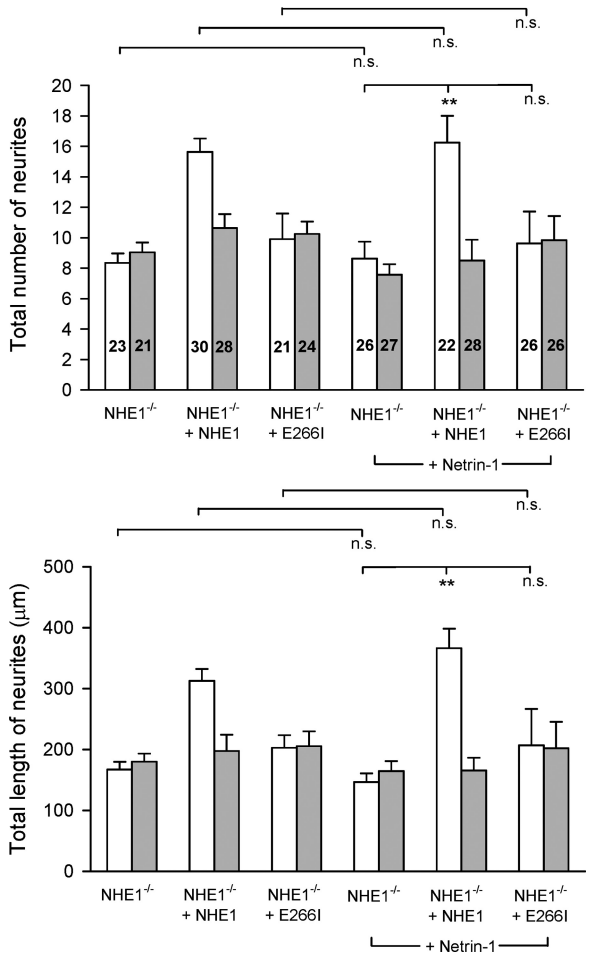

Figure 12. Netrin-1 promotes early neurite outgrowth in *NHE1*$^{-/-}$ neurons overexpressing full-length NHE1 but not NHE1–E266I. P0.5 *NHE1*$^{-/-}$ neocortical neurons were either untransfected or transiently transfected with HA-tagged full-length NHE1 (*NHE1*$^{-/-}$ + NHE1) or the ion translocation-deficient mutant NHE1–E266I (*NHE1*$^{-/-}$ + E266I) and cultured for 72 h in the absence or presence of 100 ng/ml netrin-1, as indicated in the figure, and in the absence (white bars) or presence (gray bars) of 1 μM cariporide. Experiments were conducted in parallel, all measured values are per cell, error bars represent SEM, and *n* values are shown in the columns. **$p < 0.01$; n.s., not significant ($p > 0.05$). The separated measurements of changes in the numbers and cumulative lengths of primary neurites per cell and neurite branches per cell to the total values shown are presented in supplemental Figure 8 (available at www.jneurosci.org as supplemental material).

nervous system development and potentiation of invasive cancers. Neuroscientist 14:571–583.

Brett CL, Donowitz M, Rao R (2005) Evolutionary origins of eukaryotic sodium/proton exchangers. Am J Physiol Cell Physiol 288:C223–C239.

Cardone RA, Casavola V, Reshkin SJ (2005) The role of disturbed pH dynamics and the Na^+/H^+ exchanger in metastasis. Nat Rev Cancer 5:786–795.

Chhabra ES, Higgs HN (2007) The many faces of actin: matching assembly factors with cellular structures. Nat Cell Biol 9:1110–1121.

Cirulli V, Yebra M (2007) Netrins: beyond the brain. Nat Rev Mol Cell Biol 8:296–306.

Cox GA, Lutz CM, Yang CL, Biemesderfer D, Bronson RT, Fu A, Aronson PS, Noebels JL, Frankel WN (1997) Sodium/hydrogen exchanger gene defect in slow-wave epilepsy mutant mice. Cell 91:139–148.

da Silva JS, Dotti CG (2002) Breaking the neuronal sphere: regulation of the actin cytoskeleton in neuritogenesis. Nat Rev Neurosci 3:694–704.

Denker SP, Barber DL (2002) Cell migration requires both ion translocation and cytoskeletal anchoring by the Na-H exchanger NHE1. J Cell Biol 159:1087–1096.

Denker SP, Huang DC, Orlowski J, Furthmayr H, Barber DL (2000) Direct binding of the Na-H exchanger NHE1 to ERM proteins regulates the cortical cytoskeleton and cell shape independently of H^+ translocation. Mol Cell 6:1425–1436.

Dent EW, Barnes AM, Tang F, Kalil K (2004) Netrin-1 and semaphorin 3A promote or inhibit cortical axon branching, respectively, by reorganization of the cytoskeleton. J Neurosci 24:3002–3012.

Dickens CJ, Gillespie JI, Greenwell JR (1989) Interaction between intracellular pH and calcium in single mouse neuroblastoma (N2A) and rat pheochromocytoma cells (PC12). Q J Exp Physiol 74:671–679.

Feijó JA, Sainhas J, Hackett GR, Kunkel JG, Hepler PK (1999) Growing pollen tubes possess a constitutive alkaline band in the clear zone and a growth-dependent acidic tip. J Cell Biol 144:483–496.

Flagella M, Clarke LL, Miller ML, Erway LC, Giannella RA, Andringa A, Gawenis LR, Kramer J, Duffy JJ, Doetschman T, Lorenz JN, Yamoah EN, Cardell EL, Shull GE (1999) Mice lacking the basolateral Na-K-2Cl cotransporter have impaired epithelial chloride secretion and are profoundly deaf. J Biol Chem 274:26946–26955.

Frantz C, Karydis A, Nalbant P, Hahn KM, Barber DL (2007) Positive feedback between Cdc42 activity and H^+ efflux by the Na-H exchanger NHE1 for polarity of migrating cells. J Cell Biol 179:403–410.

Frantz C, Barreiro G, Dominguez L, Chen X, Eddy R, Condeelis J, Kelly MJ, Jacobson MP, Barber DL (2008) Cofilin is a pH sensor for actin free barbed end formation: role of phosphoinositide binding. J Cell Biol 183:865–879.

Govek EE, Newey SE, Van Aelst L (2005) The role of the Rho GTPases in neuronal development. Genes Dev 19:1–49.

Grinstein S, Woodside M, Waddell TK, Downey GP, Orlowski J, Pouyssegur J, Wong DC, Foskett JK (1993) Focal localization of the NHE-1 isoform of the Na^+/H^+ antiport: assessment of effects on intracellular pH. EMBO J 12:5209–5218.

Hayashi H, Aharonovitz O, Alexander RT, Touret N, Furuya W, Orlowski J, Grinstein S (2008) Na^+/H^+ exchange and pH regulation in the control of neutrophil chemokinesis and chemotaxis. Am J Physiol Cell Physiol 294:C526–C534.

Heasman SJ, Ridley AJ (2008) Mammalian Rho GTPases: new insights into their functions from *in vivo* studies. Nat Rev Mol Cell Biol 9:690–701.

Hentschke M, Wiemann M, Hentschke S, Kurth I, Hermans-Borgmeyer I, Seidenbecher T, Jentsch TJ, Gal A, Hübner CA (2006) Mice with a targeted disruption of the Cl^-/HCO_3^- exchanger AE3 display a reduced seizure threshold. Mol Cell Biol 26:182–191.

Hisamitsu T, Ben Ammar Y, Nakamura TY, Wakabayashi S (2006) Dimerization is crucial for the function of the Na/H exchanger NHE1. Biochemistry 45:13346–13355.

Huang EJ, Reichardt LF (2001) Neurotrophins: Roles in neuronal development and function. Annu Rev Neurosci 24:677–736.

Huang WC, Swietach P, Vaughan-Jones RD, Ansorge O, Glitsch MD (2008) Extracellular acidification elicits spatially and temporally distinct Ca^{2+} signals. Curr Biol 18:781–785.

Hübner CA, Stein V, Hermans-Borgmeyer I, Meyer T, Ballanyi K, Jentsch TJ (2001) Disruption of KCC2 reveals an essential role of K-Cl cotransport already in early synaptic inhibition. Neuron 30:515–524.

Karmazyn M, Sawyer M, Fliegel L (2005) The Na^+/H^+ exchanger: a target for cardiac therapeutic intervention. Curr Drug Targets Cardiovasc Haematol Disord 5:323–335.

Keino-Masu K, Masu M, Hinck L, Leonardo ED, Chan SS, Culotti JG, Tessier-Lavigne M (1996) Deleted in Colorectal Cancer (*DCC*) encodes a netrin receptor. Cell 87:175–185.

Klein M, Seeger P, Schuricht B, Alper SL, Schwab A (2000) Polarization of Na^+/H^+ and Cl^-/HCO_3^- exchangers in migrating renal epithelial cells. J Gen Physiol 115:599–608.

Lagana A, Vadnais J, Le PU, Nguyen TN, Laprade R, Nabi IR, Noël J (2000) Regulation of the formation of tumor cell pseudopodia by the Na^+/H^+ exchanger NHE1. J Cell Sci 113:3649–3662.

Li W, Lee J, Vikis HG, Lee SH, Liu G, Aurandt J, Shen TL, Fearon ER, Guan JL, Han M, Rao Y, Hong K, Guan KL (2004) Activation of FAK and Src are receptor-proximal events required for netrin signaling. Nat Neurosci 7:1213–1221.

Li X, Saint-Cyr-Proulx E, Aktories K, Lamarche-Vane N (2002) Rac 1 and Cdc42 but not RhoA or Rho kinase activities are required for neurite outgrowth induced by the Netrin-1 receptor DCC (*D*eleted in *C*olorectal *C*ancer) in N1E-115 neuroblastoma cells. J Biol Chem 277:15207–15214.

Litvin TN, Kamenetsky M, Zarifyan A, Buck J, Levin LR (2003) Kinetic properties of "soluble" adenylyl cyclase. J Biol Chem 278:15922–15926.

Liu G, Beggs H, Jürgensen C, Park HT, Tang H, Gorski J, Jones KR, Reichardt LF, Wu J, Rao Y (2004) Netrin requires focal adhesion kinase and Src family kinases for axon outgrowth and attraction. Nat Neurosci 7:1222–1232.

Luo J, Chen H, Kintner DB, Shull GE, Sun D (2005) Decreased neuronal death in Na^+/H^+ exchanger isoform 1-null mice after *in vitro* and *in vivo* ischemia. J Neurosci 25:11256–11268.

Masereel B, Pochet L, Laeckmann D (2003) An overview of inhibitors of Na^+/H^+ exchanger. Eur J Med Chem 38:547–554.

Meima ME, Mackley JR, Barber DL (2007) Beyond ion translocation: structural functions of the sodium-hydrogen exchanger isoform 1. Curr Opin Nephrol Hypertens 16:365–372.

Ming GL, Song HJ, Berninger B, Holt CE, Tessier-Lavigne M, Poo MM (1997) cAMP-dependent growth cone guidance by netrin-1. Neuron 19:1225–1235.

Mitsui K, Yasui H, Nakamura N, Kanazawa H (2005) Oligomerization of the *Saccharomyces cerevisiae* Na^+/H^+ antiporter Nha1p: implications for its antiporter activity. Biochim Biophys Acta 1720:125–136.

Nakajima K, Miyazaki H, Niisato N, Marunaka Y (2007) Essential role of NKCC1 in NGF-induced neurite outgrowth. Biochem Biophys Res Commun 359:604–610.

Niblock MM, Brunso-Bechtold JK, Riddle DR (2000) Insulin-like growth factor I stimulates dendritic growth in primary somatosensory cortex. J Neurosci 20:4165–4176.

Orlowski J (1993) Heterologous expression and functional properties of the amiloride high affinity (NHE-1) and low affinity (NHE-3) isoforms of the rat Na/H exchanger. J Biol Chem 268:16369–16377.

Orlowski J, Grinstein S (2004) Diversity of the mammalian sodium/proton exchanger SLC9 gene family. Pflügers Arch 447:549–565.

Pantazis A, Keegan P, Postma M, Schwiening CJ (2006) The effect of neuronal morphology and membrane-permeant weak acid and base on the dissipation of depolarization-induced pH gradients in snail neurons. Pflügers Arch 452:175–187.

Pieraut S, Laurent-Matha V, Sar C, Hubert T, Méchaly I, Hilaire C, Mersel M, Delpire E, Valmier J, Scamps F (2007) NKCC1 phosphorylation stimulates neurite growth of injured adult sensory neurons. J Neurosci 27:6751–6759.

Putney LK, Barber DL (2004) Expression profile of genes regulated by activity of the Na-H exchanger NHE1. BMC Genomics 5:46.

Ren XR, Ming GL, Xie Y, Hong Y, Sun DM, Zhao ZQ, Feng Z, Wang Q, Shim S, Chen ZF, Song HJ, Mei L, Xiong WC (2004) Focal adhesion kinase in netrin-1 signaling. Nat Neurosci 7:1204–1212.

Rojas JD, Sennoune SR, Maiti D, Bakunts K, Reuveni M, Sanka SC, Martinez GM, Seftor EA, Meininger CJ, Wu G, Wesson DE, Hendrix MJ, Martínez-Zaguilán R (2006) Vacuolar-type H^+-ATPases at the plasma membrane regulate pH and cell migration in microvascular endothelial cells. Am J Physiol Heart Circ Physiol 291:H1147–H1157.

Round J, Stein E (2007) Netrin signaling leading to directed growth cone steering. Curr Opin Neurobiol 17:15–21.

Sardet C, Franchi A, Pouysségur J (1989) Molecular cloning, primary structure, and expression of the human growth factor-activatable Na/H antiporter. Cell 56:271–280.

Schneider L, Stock CM, Dieterich P, Jensen BH, Pedersen LB, Satir P, Schwab A, Christensen ST, Pedersen SF (2009) The Na^+/H^+ exchanger NHE1 is required for directional migration stimulated via PDGFR-α in the primary cilium. J Cell Biol 185:163–176.

Scholz W, Albus U, Counillon L, Gögelein H, Lang HJ, Linz W, Weichert A, Schölkens BA (1995) Protective effects of HOE642, a selective sodium-hydrogen exchange subtype 1 inhibitor, on cardiac ischaemia and reperfusion. Cardiovasc Res 29:260–268.

Schwab A, Rossmann H, Klein M, Dieterich P, Gassner B, Neff C, Stock C, Seidler U (2005) Functional role of Na^+-HCO_3^- cotransport in migration of transformed renal epithelial cells. J Physiol 568:445–458.

Shekarabi M, Kennedy TE (2002) The Netrin-1 receptor DCC promotes filopodia formation and cell spreading by activating Cdc42 and Rac1. Mol Cell Neurosci 19:1–17.

Shekarabi M, Moore SW, Tritsch NX, Morris SJ, Bouchard JF, Kennedy TE (2005) Deleted in Colorectal Cancer binding netrin-1 mediates cell substrate adhesion and recruits Cdc42, Rac1, Pak1, and N-WASP into an intracellular signaling complex that promotes growth cone expansion. J Neurosci 25:3132–3141.

Sheldon C, Church J (2002) Intracellular pH response to anoxia in acutely dissociated adult rat hippocampal CA1 neurons. J Neurophysiol 87:2209–2224.

Sheldon C, Diarra A, Cheng YM, Church J (2004) Sodium influx pathways during and after anoxia in rat hippocampal neurons. J Neurosci 24:11057–11069.

Simchowitz L, Cragoe EJ Jr (1986) Regulation of human neutrophil chemotaxis by intracellular pH. J Biol Chem 261:6492–6500.

Simons M, Gault WJ, Gotthardt D, Rohatgi R, Klein TJ, Shao Y, Lee HJ, Wu AL, Fang Y, Satlin LM, Dow JT, Chen J, Zheng J, Boutros M, Mlodzik M (2009) Electrochemical cues regulate assembly of the Frizzled/Dishevelled complex at the plasma membrane during planar epithelial polarization. Nat Cell Biol 11:286–294.

Song H, Poo M (2001) The cell biology of neuronal navigation. Nat Cell Biol 3:E81–E88.

Srivastava J, Barber DL, Jacobson MP (2007) Intracellular pH sensors: design principles and functional significance. Physiology 22:30–39.

Srivastava J, Barreiro G, Groscurth S, Gingras AR, Goult BT, Critchley DR, Kelly MJ, Jacobson MP, Barber DL (2008) Structural model and functional significance of pH-dependent talin-actin binding for focal adhesion remodeling. Proc Natl Acad Sci U S A 105:14436–14441.

Stock C, Cardone RA, Busco G, Krähling H, Schwab A, Reshkin SJ (2008) Protons extruded by NHE1: digestive or glue? Eur J Cell Biol 87:591–599.

Stüwe L, Müller M, Fabian A, Waning J, Mally S, Noël J, Schwab A, Stock C (2007) pH dependence of melanoma cell migration: protons extruded by NHE1 dominate protons of the bulk solution. J Physiol 585:351–360.

Tang F, Kalil K (2005) Netrin-1 induces axon branching in developing cortical neurons by frequency-dependent calcium signaling pathways. J Neurosci 25:6702–6715.

Tombaugh GC, Somjen GG (1998) pH modulation of voltage-gated ion channels. In: pH and brain function (Kaila K, Ransom BR, eds), pp 395–416. New York: Wiley.

Traynelis SF (1998) pH modulation of ligand-gated ion channels. In: pH and brain function (Kaila K, Ransom BR, eds), pp 417–446. New York: Wiley.

Vaughan-Jones RD, Spitzer KW, Swietach P (2006) Spatial aspects of intracellular pH regulation in heart muscle. Prog Biophys Mol Biol 90:207–224.

Vaughan-Jones RD, Spitzer KW, Swietach P (2009) Intracellular pH regulation in heart. J Mol Cell Cardiol 46:318–331.

Wang GX, Poo MM (2005) Requirement of TRPC channels in netrin-1-induced chemotropic turning of nerve growth cones. Nature 434:898–904.

Willoughby D, Thomas R, Schwiening C (2001) The effects of intracellular pH changes on resting cytosolic calcium in voltage-clamped snail neurons. J Physiol 530:405–416.

Willoughby D, Masada N, Crossthwaite AJ, Ciruela A, Cooper DMF (2005) Localized Na^+/H^+ exchanger 1 expression protects Ca^{2+}-regulated adenylyl cyclases from changes in intracellular pH. J Biol Chem 280:30864–30872.

Wu KL, Khan S, Lakhe-Reddy S, Jarad G, Mukherjee A, Obejero-Paz CA, Konieczkowski M, Sedor JR, Schelling JR (2004) The NHE1 Na^+/H^+ exchanger recruits ezrin/radixin/moesin proteins to regulate AKT-dependent cell survival. J Biol Chem 279:26280–26286.

Xia Y, Zhao P, Xue J, Gu XQ, Sun X, Yao H, Haddad GG (2003) Na^+ channel expression and neuronal function in the Na^+/H^+ exchanger 1 null mutant mouse. J Neurophysiol 89:229–236.

Xue J, Douglas RM, Zhou D, Lim JY, Boron WF, Haddad GG (2003) Expression of Na^+/H^+ and HCO_3^--dependent transporters in Na^+/H^+ exchanger isoform mutant mouse brain. Neuroscience 122:37–46.

Xue J, Zhou D, Yao H, Gavrialov O, McConnell MJ, Gelb BD, Haddad GG (2007) Novel functional interaction between Na^+/H^+ exchanger 1 and tyrosine phosphatase SHP-2. Am J Physiol Regul Integr Comp Physiol 292:R2406–R2416.

Yao H, Ma E, Gu XQ, Haddad GG (1999) Intracellular pH regulation of CA1 neurons in Na^+/H^+ isoform 1 mutant mice. J Clin Invest 104:637–645.

Zhou D, Xue J, Gavrialov O, Haddad GG (2004) Na^+/H^+ exchanger 1 deficiency alters gene expression in mouse brain. Physiol Genomics 18:331–339.